Characterization of Chemical Libraries for Luciferase Inhibitory Activity

Douglas S. Auld,[†] Noel T. Southall,[†] Ajit Jadhav,[†] Ronald L. Johnson,[†] David J. Diller,[‡] Anton Simeonov,[†] Christopher P. Austin,[†] and James Inglese*,[†]

NIH Chemical Genomics Center, National Human Genome Research Institute, National Institutes of Health, Bethesda, Maryland 20892-3370, and Pharmacopeia Inc., Princeton, New Jersey 08543

Received October 16, 2007

To aid in the interpretation of high-throughput screening (HTS) results derived from luciferase-based assays, we used quantitative HTS, an approach that defines the concentration−response behavior of each library sample, to profile the ATP-dependent luciferase from *Photinus pyralis* against more than 70 000 samples. We found that approximately 3% of the library was active, containing only compounds with inhibitory concentration−responses, of which 681 (0.9%) exhibited IC_{50} < 10 μM. Representative compounds were shown to inhibit purified *P. pyralis* as well as several commercial luciferase-based detection reagents but were found to be largely inactive against *Renilla reniformis* luciferase. Light attenuation by the samples was also examined and found to be more prominent in the blue-shifted bioluminescence produced by *R. reniformis* luciferase than in the bioluminescence produced by *P. pyralis* luciferase. We describe the structure−activity relationship of the luciferase inhibitors and discuss the use of this data in the interpretation of HTS results and configuration of luciferase-based assays.

Introduction

Bioluminescence occurs in a variety of organisms and serves primarily as defense and communication means; the color of luminescence is adapted to the visual systems of the organism.[1] Bioluminescence colors can range from blue to red (Figure 1a). The particular wavelength that is emitted depends in part on the type of luciferins that is employed, and these cover diverse structural classes (Figure 1a).[2] Luciferases from organisms that yield very bright bioluminescence have been adapted for use as reporters in high-throughput screening (HTS)[a] assays, the most common being from the jellyfish *Aequorea victoria*, the sea pansy *Renilla reniformis*, and the firefly *Photinus pyralis*.

Firefly luciferase enables a variety of HTS applications, including reporters for gene expression in cellular signaling assays, sensors for the ATP content of cells as a measure of cell viability, and in biochemical assays to measure both ATP-dependent enzyme reactions, such as kinases, and non-ATP-dependent enzymes, such as the cytochrome P450 (CYP) family of oxidoreductases by using pro-luciferin CYP substrates.[3] The active site of firefly luciferase binds ATP and a luciferin containing a benzthiazole core. The bioluminescent reaction proceeds through the formation of a luciferyl−adenylate intermediate and leads to the production of AMP, oxyluciferin, and light (Figure 1b).[4] The environment of the active site also

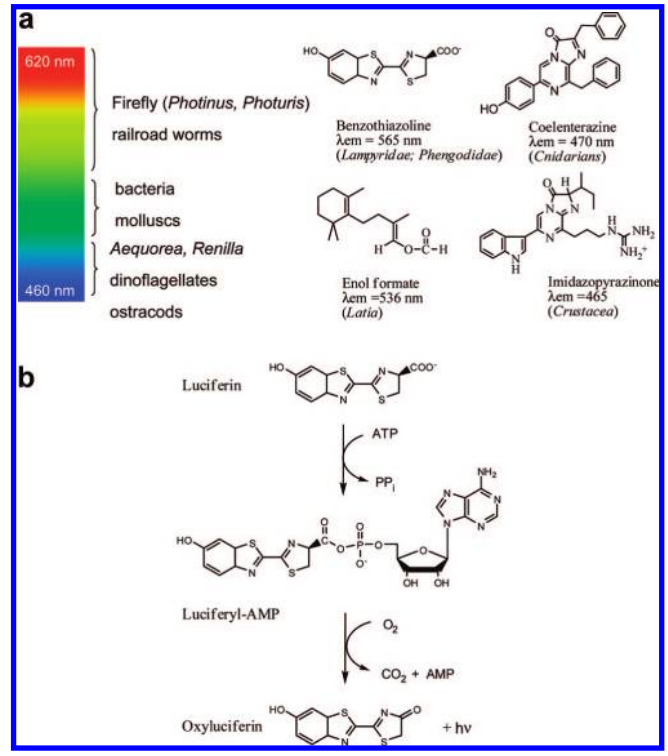

Figure 1. Bioluminescence of the luciferyl−luciferase reaction. (a) The spectrum of bioluminescence is shown at left along with the names of the organisms that produce the luminescence. Also shown at right are luciferins for firefly (*Lampryridae*) and railroad worms (*Phengodidae*), sea pansies and jellyfish (*Cnidarians*), mollusks (*Latia*), and ostracods (*Crustacea*; the ostracod *Cypridina (Vargula) hirgendorfii*). (b) Enzymatic reaction of *Photonis* luciferase. Luciferin and adenosine 5′-triphosphate (ATP) substrates are used by luciferase to form a luciferyl−adenosine 5′-monophosphate (AMP) intermediate that is subsequently oxidized in the presence of oxygen to generate light, as well as the products oxyluciferin, CO_2, and AMP.

* To whom correspondence should be addressed. E-mail: jinglese@mail.nih.gov. Phone: 301-217-5723. Fax: 301-217-5736.

† National Institutes of Health.

‡ Pharmacopeia Inc.

[a] Abbreviations: IC_{50}, determined by using the detection cocktail from PK-Light; IC_{50Luc}, determined by using purified *P. pyralis* luciferase; $IC_{50Promega}$, determined by using the detection cocktail from Kinase-Glo; $IC_{50SteadyGlo}$, determined by using the reporter gene formulation SteadyGlo and purified *P. pyralis* luciferase; $IC_{50BrightGlo}$, determined by using the reporter gene formulation BrightGlo and purified *P. pyralis* luciferase; $IC_{50Renilla}$, determined by using purified *R. reniformis* luciferase; HTS, high-throughput screening; AMP, adenosine 5′-monophosphate; ATP, adenosine 5′-triphosphate; qHTS, quantitative high-throughput screening; BSA, bovine serum albumin; DMSO, dimethylsulfoxide; NCGC, NIH Chemical Genomics Center; SD, standard deviation; AID, Assay Identifier number for PubChem; MCS, maximal common substructures; CID, Compound Identifier number for PubChem; Z′, a score of assay performance measured in the absence of test compounds where values between 0.5 and 1.0 represent acceptable assays; MW, molecular weight; BEH, bridged ethyl hybrid; LCMS, liquid chromatography–mass spectrometry; ELSD, evaporative light scattering detection; EGFR, epidermal growth factor receptor.

10.1021/jm701302v CCC: $40.75
Published on Web 03/26/2008

influences the wavelength of the light emitted, and single amino acid changes within the active site of *P. pyralis* luciferase can shift the luminescence from yellow-green to red.[5]

Because firefly luciferase is used as a detection reagent in cell- and protein-based assays, it is widely appreciated that compounds may interfere with this detection through a variety of mechanisms.[6] These include direct inhibition of the enzyme by specific competition with one or both substrates and nonspecific inhibition, as for example, enzyme denaturation or attenuation of the luminescent signal through photonic processes such as absorbance or the inner-filter effect.[7] Although not described in the literature, luciferase assay interference has been identified within industrial HTS laboratories by accumulating numerous data sets from luciferase-based screens and then by using this information to flag compounds that are frequently active in this mode of detection. However, compounds that are active against luciferase may also be genuinely active against the target of interest. For instance, resveratrol[8,9] is a potent luciferase inhibitor that complicates the interpretation of data collected from luciferase-based reporter gene assays for this compound.[10] Such observations emphasize the need to understand luciferase inhibition by small molecules when these are characterized in common luciferase-based assays, particularly those that measure cytotoxic effects where a misinterpretation of the data could result in discarding useful leads.

A counter-screen database to flag assay interferences, such as luciferase inhibition, would be very useful, but no such database is currently publicly available. We therefore investigated the frequency and type of compounds that have activity against firefly luciferase within a set of publicly accessible compounds. We employed a concentration−response-based screening strategy, termed quantitative high-throughput screening (qHTS),[11] that produced potency values for approximately 72 000 compounds (see PubChem AID 411). The active structures and series identified can be used to refine and gain information on the selection of actives obtained from many commonly used luciferase-based assays. Also, we suggest a model for how substrate-competitive inhibitors identified here may bind in the luciferase active site, and how differences in ATP binding between protein kinases and firefly luciferase may influence the interpretation of inhibitors derived from luciferase-coupled protein kinase assays. On the basis of these data, several approaches to the design of luciferase assays are suggested that should improve these assays by reducing the potential for compound interference.

Material and Methods

Reagents. ATP, bovine serum albumin (BSA), Tween 20, potassium chloride, imidazole, resveratrol, D-luciferin, and apigenin were purchased from Sigma-Aldrich (St. Louis, MO). Magnesium chloride was acquired from Quality Biological (Gaithersburg, MD), and dimethylsulfoxide (DMSO), certified ACS grade, was purchased from Fisher (Waltham, MA). *R. reniformis* luciferase was purchased from Chemicon International (cat. no. 4400). The luciferase-based detection reagents used were PK-Light (Lonza, Allendale, NJ), EasyLite (Perkin-Elmer, Waltham, MA), and Kinase-Glo (Promega, Madison, WI). The luciferase reporter gene reagents used were SteadyGlo and BrightGlo (Promega). Purified wild-type *P. pyralis* luciferase was obtained from Sigma (cat. no. L9506).

Preparation of Compound Libraries and Control Plates. The 72 377-member library was collected from several sources: 1280 compounds from Sigma-Aldrich (LOPAC1280), 1120 compounds from Prestwick Chemical Inc. (Illkirch, France), 280 purified natural products from TimTec (Newark, DE), three 1000-member combinatorial libraries from Pharmacopeia (Cranbury, NJ), 977 compounds from Tocris (Ellisville, MO), 63 021 compounds from the NIH Molecular Libraries Small Molecule Repository,[12] 1981 compounds from the National Cancer Institute, and 718 compounds from Boston University Center for Chemical Methodology and Library Development. Libraries were prepared as described.[11,13] Controls were added from a separate 1536-well compound plate as follows: columns 1 and 2, 16-point titrations in duplicate of resveratrol and apigenin, respectively (both beginning at 20 mM in DMSO); column 3, neutral control (DMSO); column 4, control inhibitor (20 mM resveratrol).

Luciferase Assay and qHTS. A total of 2 μL/well of substrate/buffer concentrate (10 μM ATP, 50 mM KCl, 7 mM $MgCl_2$, 0.05% BSA, 0.01% Tween 20, and 50 mM imidazole pH 7.2, final concentration) was dispensed into Kalypsys (San Diego, CA) solid white 1536-well plates by using a bottle-valve solenoid-based dispenser (Kalypsys). A total of 23 nL of compound solution was transferred to the assay plate by using a Kalypsys pin tool equipped with a 1536-pin array[14] containing 10 nL slotted pins (FP1S10, 0.457 mm diameter, 50.8 mm long; V&P Scientific, San Diego, CA). After transfer, 2 μL/well of PK-Light (resuspended in buffer B described in ref 15) was dispensed for a final assay volume of 4 μL/well. After an 8 min incubation at ambient temperature, luminescence was detected by a ViewLux (Perkin-Elmer) by using a 5 s exposure time and 1X binning. All screening operations were performed by using a fully integrated Kalypsys robotic system containing one RX-130 and two RX-90 Staübli anthropomorphic robotic arms.

qHTS Data Analysis. Screening data were processed by using in-house-developed software. Percent activity was computed from the median values of the uninhibited, or neutral, control (32 wells located in column 3) and the 20 μM resveratrol, or 100% inhibited, control (32 wells, column 4). For assignment of plate concentrations and sample identifiers, ActivityBase (ID Business Solutions Ltd., Guildford, UK) was used for compound and plate registrations. An in-house database was used to track sample concentrations across plates. Correction factors were generated from 18 control assay plates containing vehicle (DMSO) only that were inserted uniformly throughout the screen to monitor background systematic variation in assay signal, potentially resulting from reagent dispensers or decreases in enzyme-specific activity, for example. Curve fitting was performed by using an in-house-developed algorithm. A four-parameter Hill equation was fitted to the concentration−response data by minimizing the residual error between the modeled and observed responses. The noise of the assay was estimated by calculating the standard deviation (SD) of the activity values obtained at the lowest tested compound concentration, and outliers were identified and masked by modeling the Hill equation and determining whether the differences exceeded the assay noise. qHTS data was depicted by using Origin (OriginLab, Northampton, MA). Data were deposited in PubChem (AID 411).

SAR Analysis. The curve classification used is the same as the one described elsewhere.[11] Briefly, concentration−response curves are categorized into four classes. Class 1 contains complete concentration−response curves showing both upper and lower asymptotes and r^2 values greater than 0.9. Class 2 contains incomplete concentration−response curves lacking the lower asymptote and shows r^2 values greater than 0.9. Class 3 curves are of the lowest confidence because they are defined by a single concentration point where the minimal acceptable activity is set at 3 SD of the mean activity calculated as described above. Curves are classified as negative or positive, depending on whether they exhibit a signal decrease (apparent inhibition) or increase (apparent activation). Finally, class 4 contains compounds that do not show any concentration−response curves and are therefore classified as inactive. Active compounds were identified as a range of curve classes from −1 through −3 to select for compounds showing signal decreases. Once an active set of compounds was identified, hierarchical agglomerative clustering with a 0.7 Tanimoto cutoff was performed by using Leadscope (Leadscope Inc., Columbus, OH) fingerprints, which are ideally suited for two-dimensional scaffold-based clustering. For each cluster, maximal common substructures (MCS) were extracted, a manual step of MCS

trimming was performed to create a list of scaffolds, and any overlapping scaffolds were abridged to a canonical set. Each scaffold was then represented as a precise definition to indicate descriptors such as the number of attachment points or the ring size variability. All filters were then relaxed to include the entire negative (i.e., class 4) assay data.

Analytical QC of Compounds. The entire library was subjected to purity analysis before plating (Galapagos Biofocus DPI, South San Francisco, CA).[16] Active compounds that were obtained from commercial sources were reanalyzed for purity. For these resupplied compounds, the purity analysis was performed via liquid chromatography−mass spectrometry (LCMS) analysis on a Waters ACQUITY reverse-phase UPLC system and a 1.7 M BEH column (2.1 × 50 mm) by using a linear gradient in 0.1% aqueous formic acid (5% ACN in water increasing to 95% over 3 min). Compound purity was measured on the basis of peak integration from both UV/vis absorbance and evaporative light scattering detection (ELSD), and compound identity was determined on the basis of mass analysis; all compounds passed purity criteria (>95%).

Follow-up Luciferase Assays. A total of 46 compounds were obtained and subjected to several luciferase assays by using a 1536-well plate format including the qHTS PK-Light detection conditions. The same buffer as the one described for the qHTS assay protocol was used for additional detection reagents, except that 2 μL of either EasyLite or Kinase-Glo was added for detection. Firefly luciferase was assayed in the qHTS assay buffer by using *P. pyralis* luciferase and D-luciferin at final concentrations 10 nM and 10 μM, respectively. This assay system was also used to vary both ATP and D-luciferin concentrations.

Luciferase reporter gene reagents (SteadyGlo and BrightGlo) were assayed by using 5 nM purified *P. pyralis* luciferase (Sigma) with no additional ATP or D-luciferin added. Activity against *R. reniformis* was assayed in 50 mM NaCl, 0.05% BSA, 0.01% Tween 20, and 50 mM Tris-acetate pH 7.2 buffer by using 10 nM *R. reniformis* luciferase and 10 μM coelentrazine. All follow-up concentration−response curves were derived from 16 2-fold concentrations. Each compound was assayed in duplicate, and this experiment was repeated on two or three separate days.

Light Attenuation Assay. Experiments to assess the luminescent-light attenuation (e.g., light-absorbing or inner-filter effects) of compounds were performed by using a Fluoromax-4 (Horiba Jobin Yvon, Edison, NJ) spectrofluorometer equipped with a single-cuvette sample holder. Assays were performed at room temperature by using two-chamber Spectrosil Far UV quartz cuvettes (Starna Cells, Atascadero, CA). To observe the luminescence from a luciferyl−luciferase reaction mixture alone, the cuvette was placed in the sample holder such that the enzyme reaction was facing the detector. For measurement of the light-attenuation effect of test compounds, the second compartment was filled with the same volume (800 μL) of compound solution in matching buffer, and the cuvette was placed in the holder with the compound compartment being situated between the luciferase-containing compartment and the light detector. Thus, the luciferase-only and compound-attenuated signals were measured in rapid succession by simply flipping the cuvette and exposing the respective compartments to the detector face. In order to measure unattenuated luminescence on this instrument, the excitation monochromator was tuned to an IR frequency (1000 nm), and the excitation slit width was decreased to a minimum (0.1 nm). At these settings, the background (buffer- or substrate-only samples in the same cuvette) remained constant from day-to-day at 160−190 cps (photon counts per second), whereas the measured values from the different experiments performed were generally between 10^4 and 5×10^6 cps. The light emitted from the samples was measured as an emission scan generally between 400 and 700 nm, at monochromator wavelength steps of 2 nm and integration time of 0.1 s. The *P. pyralis* firefly luciferase reaction used 100 μM ATP and D-luciferin with 100 nM enzyme, and the *R. reniformis* reaction used 50 μM coelentrazine and 100 nM enzyme; the buffers described above were used for the follow-up assays. Compounds were titrated by 2-fold dilutions starting at a concentration of 100 μM until no quenching was observed. The emission slit width was 5 nm for the firefly luciferase assays and 10 nm for the *R. reniformis* experiments.

Modeling of Luciferase Inhibitor. Modeling of substrate competitive inhibitors and comparison of ATP binding between a protein kinase and luciferase was performed by using the luciferase protein from Japanese firefly (PDB code 2D1R)[5] and the epidermal growth factor receptor (EGFR) protein kinase, cocrystalized with a 4-anilinoquinazoline inhibitor or an ATP analogue (PDB codes 1M17[17] and 2GS7,[18] respectively). The Japanese firefly structure was chosen because it was solved in complex with both oxyluciferin and AMP. The Japanese firefly and *P. pyralis* luciferase show high overall sequence similarity (68% identity and 82% similarity with only a single amino acid gap), and their binding sites are nearly perfectly conserved. We therefore reasoned that the Japanese firefly structure is an acceptable model for luciferase bound to substrates or inhibitors in either the AMP- or luciferin-binding site. All inhibitor-binding models were built manually starting from either of the cocrystallized substrates in the structure 2D1R and were further optimized by using MOE (Molecular Operating Environment, 2006).

Results

Luciferase qHTS. To profile the chemical library for activity against luciferase, the luciferase enzyme from *P. pyralis* was assayed by using a commercially available detection system containing enzyme, luciferin, and buffer components.[15] The enzyme activity was linear over a range of 5−20 μM of ATP, and 10 μM was chosen for the assay. The screen was performed in a 1536-well plate format with a final assay volume of 4 μL per well. Resveratrol and apigenin, luciferase inhibitors identified through a counter-screen of pyruvate kinase actives,[11] were used as inhibitor controls.

Luciferase activity was screened against small molecules by using a concentration−response method (qHTS).[11] Unlike traditional HTS, where libraries are tested at a single concentration, qHTS measures activity across multiple concentrations allowing the generation of titration−response curves for all library compounds. In the luciferase qHTS, the library was tested as a series of at least seven 5-fold dilutions beginning at a concentration of 57 μM for ∼85% of the compounds and 25 or 11 μM for the remainder.

A total of 441 1536-well microtiter plates were processed. The 426 plates accepted for further analysis averaged a signal-to-background ratio of 7.9 ± 0.9 and $Z' = 0.85 \pm 0.08$, indicating a strong and consistent assay response over the entire screen. During the run, a dispenser tip was partially blocked for 16 plates, which caused lower Z' values (0.18−0.59) and 20% lower activity for the affected compounds (Figure 2A). The inhibitor control titrations included on every plate were highly precise, and the minimum significance ratios (MSR, minimum significance ratio that represents the smallest potency ratio between two measurements that is statistically significant with 95% confidence)[19] for resveratrol and apigenin were 1.8 and 1.6, respectively (Figure 2B).

The luciferase qHTS resulted in titration−response profiles of 72 377 samples derived from 654 336 assayed wells (Figure 2A). Screening was performed at a rate of 6.6 samples/s on the Kalypsys automated screening platform, thus generating data for one concentration−response curve per second. Concentration−response curves were fitted to the data corresponding to each sample and categorized into four classes: (1) complete response curves containing upper and lower asymptotes, (2) incomplete response curves having an upper asymptote, (3) poorly fit curves or activity only at the highest tested concentration, and (4) inactive where activity was below 30%.[11]

The screen identified 2311 samples comprising 3.1% of the library as active (classes 1−3) and 70 061 as inactive (class 4).

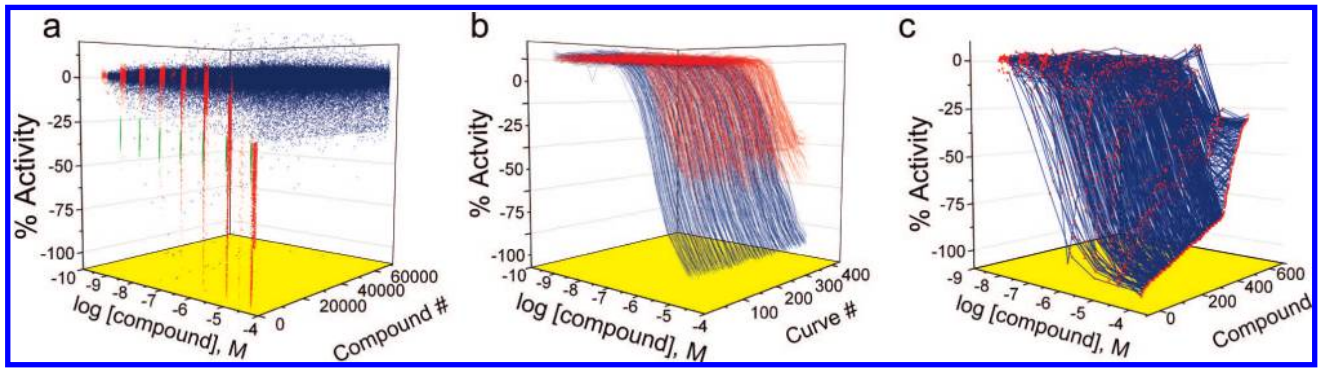

Figure 2. Luciferase qHTS. (a) Concentration−response data are shown for active (red) and inactive (blue) compounds. Activities for 352 compounds (green) were reduced because of a partially occluded reagent dispenser tip. (b) Titration−response curves for the control luciferase inhibitors, resveratrol (blue) and apigenin (red). (c) Representation of class 1 concentration−response curves derived from the qHTS. Data points are shown in red with blue wire-frames drawn through the points to represent the concentration−response curves.

Table 1. Analysis of qHTS

	curve classification					
IC_{50} (μM)	**1a**	**1b**	**2a**	**2b**	**3**	**total**
<0.1	5	0	0	0	0	5
0.1−1	58	15	0	2	5	80
1−10	146	121	176	104	49	596
10−100	0	0	71	1058	261	1390
>100	0	0	0	131	109	240
total per classification	209	136	247	1295	424	2311
% of library	0.29	0.19	0.34	1.79	0.59	3.19

All actives were inhibitors. Compounds associated with the highest quality curves, classes 1a, 1b, and 2a, comprising 209, 136, and 247 samples, respectively, represented 0.8% of the collection (Figure 2C). Class 2b was the largest class of actives, containing 1295 samples, whereas class 3 totaled 424 samples.

The luciferase qHTS tested compound activities at concentrations from 3.7 nM to as high as 57 μM. We estimated that the luciferase concentration was ~1 nM in the assay,[15] indicating that our determination of inhibitor IC_{50} should be accurate because the enzyme concentration was below the lowest tested compound concentration. The distribution of potencies for each curve class indicated that, as expected, the mean IC_{50} increased with decreasing curve class quality (Table 1). The class 1a category contained the most potent inhibitor, and IC_{50} values ranged from 0.04 to 5 μM, whereas class 1b potencies spanned from 0.25 to 8 μM. The potencies of class 2 compounds were lower, class 2a and 2b compounds having $IC_{50} \geq 1.3$ μM and $IC_{50} \geq 0.4$ μM, respectively. Many class 2b and 3 IC_{50} values were above the highest tested concentration; these were extrapolated from incomplete curves; therefore, they should be considered approximations.

Luciferase SAR. Active library members with high-confidence curve classes (1a, 1b, and 2a) were selected and subjected to hierarchical clustering by using Leadscope fingerprints to generate MCS. Seven chemotypes were chosen for further analysis on the basis of the number of analogues associated with the MCS, potency of these analogues, and known biological information associated with the compounds (see Figure 3 for core structures). For example, the most highly representative structures observed from this analysis were the 2 aryl-substituted benzo-[d]thiazole, -imidazole, and -oxazole-containing series, likely analogues of the benzthiazole-based luciferin substrate. We also selected four clusters that did not show obvious similarity to either luciferin or ATP, represented by a set of 1,2,4-oxadiazoles, a series of quinoline compounds, and several compounds with a substituted (*Z*)-(amino)prop-2-en-1-one core or benzlyamide core, as well as compounds with known pharmacological activity. Substructure searches against the entire library were performed by using the scaffolds that defined each of these clusters in order to define a chemical series composed of active and inactive analogues.

We next examined the bioactivity profile for active compounds found within each chemical series across 39 qHTS assays performed at the NCGC. These included six luciferase-based assays and 33 assays that used fluorescence detection involving reporters such as GFP or β-lactamase, or reagents such as protease profluorescent peptide substrates. On average, three-quarters of the active compounds in each cluster identified from the luciferase qHTS were found to be active in all six luciferase assays, whereas the activity averaged only 10% across the 33 nonluciferase-based assays (Figure 3). Luciferase-coupled enzyme assays that used the same luciferase-based detection reagent showed the highest degree of correlation (Figure 3a−g, first two dark gray bars, qHTS assays 1 and 2). Within each luciferase active series, the fraction of active compounds was often found to be >50% for luciferase assays with a cell-based format, and the unrelated red-luminescence-emitting click beetle luciferase showed the lowest activity for each series. In some series, the fraction of active compounds was found to be ~50% in nonluciferase assays; for example, a series containing core **4** (quinoline, Figure 3d, qHTS assays 12 and 13) was active in two fluorescence-based enzyme assays. The activity in these two assays was associated with lower-confidence curve classes (e.g., class 3) and gave rise to activation of the assay signal. Therefore, for these fluorescence-based assays, the activity of quinoline compounds appears to be due to sample fluorescence (for further discussion of fluorescent compound interference see ref 20). We next wished to understand the range of activity these compounds displayed against various luciferase-based assay formats and the nature of this inhibition.

Benzthiazole Series. We chose to focus on a set of benzthiazole compounds because of the high similarity to the 2-(4,5-dihydrothiazol-2-yl)benzo[d]thiazole core of luciferin (Figure 1). Compounds containing core **1** (benzthiazole, Figure 3) were one of the largest chemical series with 89 active analogues and 524 inactive analogues (Figure 4a). The potency of the active analogues covered a large range, the most potent compound approaching 100 nM, and many showing class 1 concentration−response curves (Figure 4a). Compounds containing core **2** (benzimidazole, Figure 3) or **3** (benzoxazole, Figure 3) were less active, and core **2** contained more actives of broader potency than core **3** (compare Figure 4b and c). Also, core **3** showed a

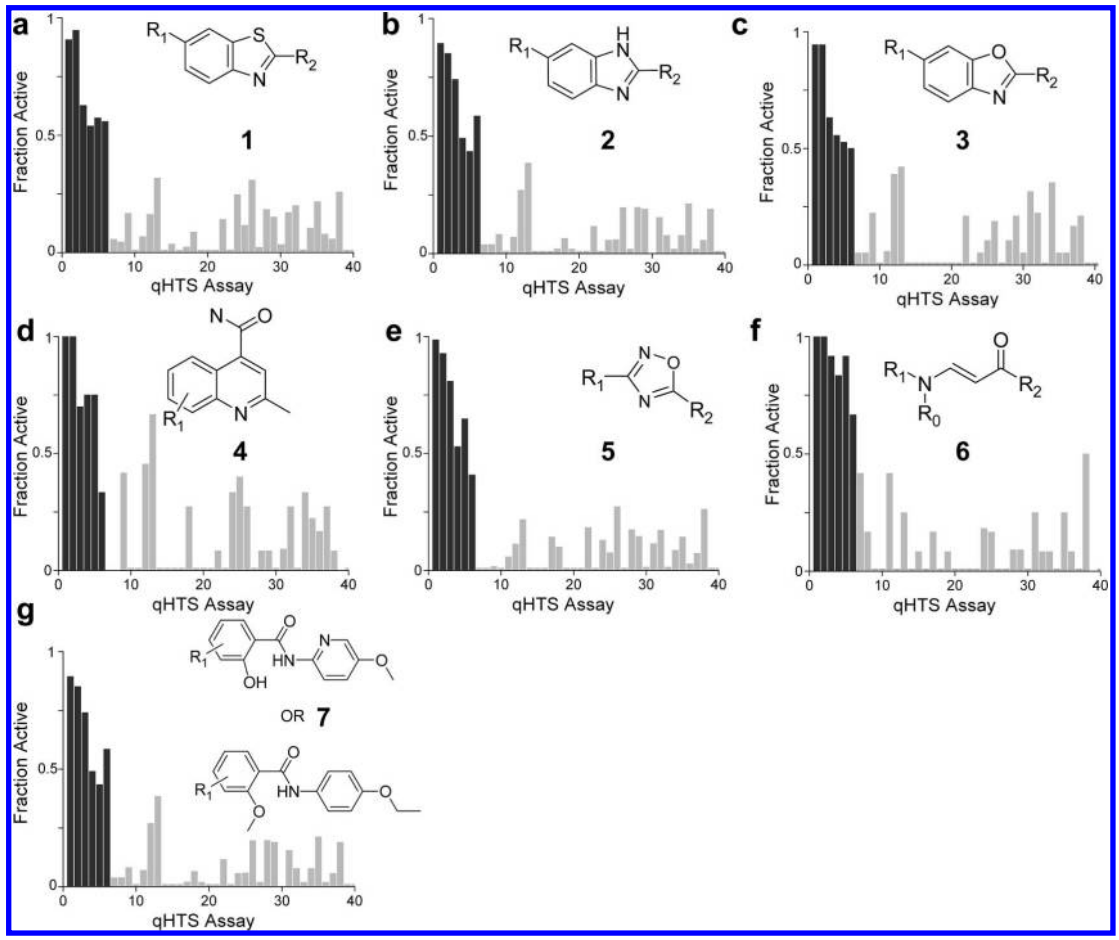

Figure 3. Bioactivity profile of the major chemical series. The activity across 39 different qHTS assays is shown for the active (i.e., qHTS classification 1−3) compounds from each chemical series identified in the luciferase qHTS (a−g). The fraction of compounds from each cluster that was active in each assay is shown. The luciferase-based assays are shown as dark gray bars at the left of each plot, and the nonluciferase-based assays are shown as light gray bars. qHTS assays 1 and 2, luciferase-coupled biochemical assays; 3−5, cell-based firefly luciferase reporter assays; 6, cell-based red emitting luciferase from click beetle *Pyrophorus plagiophthalamus* reporter assay.[36]

flatter potency distribution, exhibiting mainly class 2 curves, compared to either core **1** or **2**.

Representative active analogues containing core **1** identified in the qHTS were obtained and tested for assay-format sensitivity in several commonly used luciferase detection kits and against purified *P. pyralis* luciferase or *R. reniformis* luciferase (Table 2) to examine selectivity. Compounds **1a**−**h** inhibited all the common firefly-based detection formats, except the Promega Kinase-Glo reagent, for which we observed reduced inhibition for these compounds in several instances. Kinase-Glo utilizes a different firefly luciferase (*Photuris pennsylvanica*) mutated for improved HTS performance and stability (Promega, personal communication). Wild-type *P. pennsylvanica* shows 48.7% identity (~68% similarity) to *P. pyralis*,[21,22] and therefore, the reduced activity observed here is not surprising. However, variation of the R_2 position modulated selectivity against the *P. pennsylvanica* luciferase in some cases. For example, compound **1b** (CID 1225609) containing 5-methylthiophene at position R_1 is inactive at a 57 μM testing concentration, whereare the des-methyl analogue (**1a**, CID 670282) showed an $IC_{50} \approx 10$ μM ($IC_{50Promega}$, Table 2). Furthermore, compounds **1d** (CID 887167) and **1e** (CID 1245272) containing the 2-methlyfuran moiety at R_1 showed appreciable inhibitory activity against this detection reagent ($IC_{50Promega} \approx 4$ μM). This finding suggests that large-scale screening with *P. pennsylvanica* firefly luciferase would identify inhibitors with a different SAR than what is described here for *P. pyralis*.

To probe the mode of inhibition, we measured the IC_{50} for compounds shown in Table 2 at various ATP and luciferin substrate concentrations. Accordingly, compounds **1a**−**f** were found to be luciferin antagonists, because increasing the luciferin to 1 mM abolished the inhibition, whereas increasing ATP only marginally affected the inhibition by using a K_m level of luciferin (see Figure 5a for example). We also observed reduced inhibition when purified luciferase was added to the reporter gene reagents ($IC_{SteadyGlo}$ and $IC_{50BrightGlo}$, Table 2) in comparision to an assay that used purified luciferase, and K_m levels of substrates (IC_{50Luc}, Table 2) suggesting reporter gene formulations use high concentrations of luciferase substrates. However, for the most potent compounds analyzed in this series. compound **1g** (CID 2350207) and compound **1h** (CID 727725), we noted that this strict dependence on luciferin substrate concentration disappeared, and the potency showed only marginal shifts at high substrate concentrations. For example, compound **1g** inhibition depended on ATP in addition to luciferin concentration. In contrast, the IC_{50} of compound **1h** varied slightly from 0.3 to 1 μM at K_m vs saturating luciferin and ATP levels, respectively (data not shown). Interestingly, compound **1h** had appreciable activity in the *P. pennsylvanica* firefly reagent cocktail, whereas its inactivity against *R. reniformis* luciferase implies a nonspecific effect, such as light attenuation, as a mechanism of compound **1h** inhibition. The R_2 group of compound **1h** can act to modulate potency but also changes inhibition mode, possibly via interactions that exclude

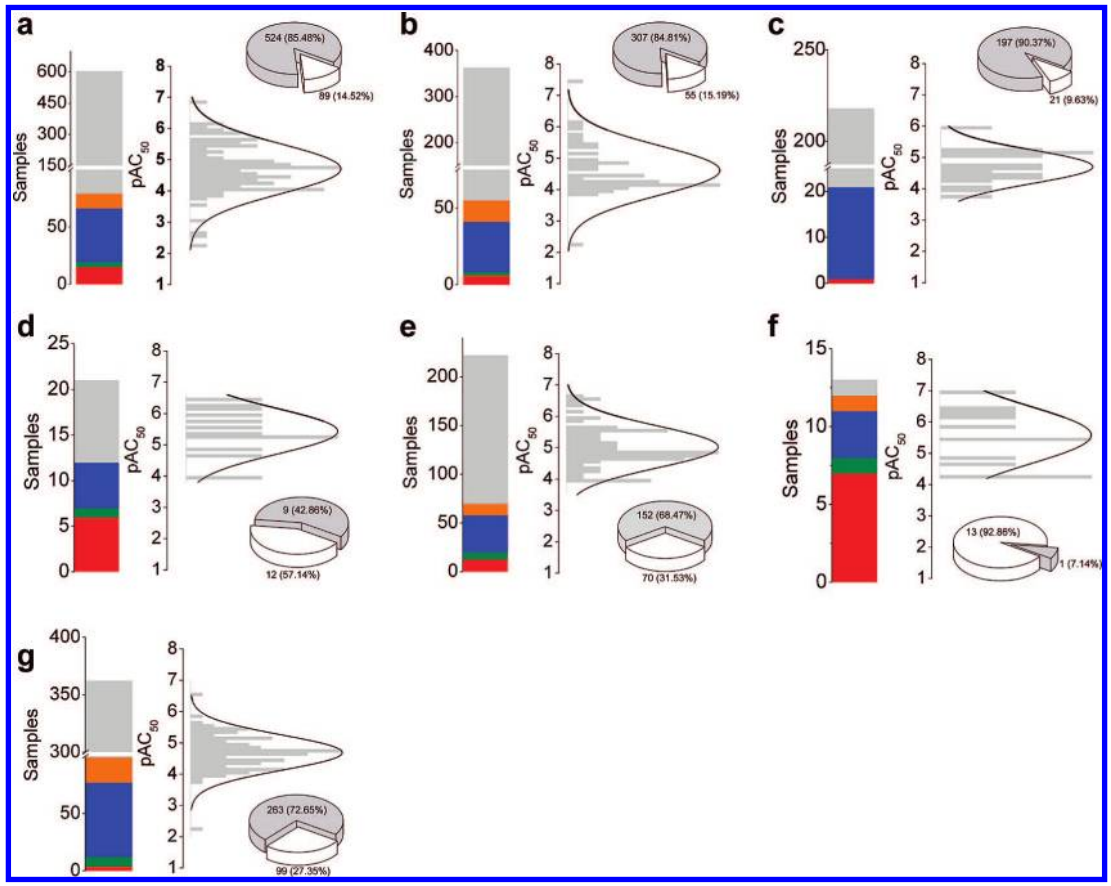

Figure 4. Pharmacological profile of the major chemical series. (a−g) Curve class and potency distribution of the seven chemical series identified in the luciferase qHTS. Curves corresponding to class 1a (red), class 1b (green), class 2 (blue), class 3 (orange), and class 4 (light gray) are depicted in the bar charts. The proportions of active curve classes 1–3 (white) and the inactive class 4 (light gray) are indicated in the pie charts. To represent the range and average activity of a series, a normal distribution fit was calculated by using Origin software on the basis of the maximum, minimum, and mean of the activity data. The chemical series shown are (a) benzthiazole (**1**), (b) benzimidazole (**2**), (c) benzoxazole (**3**), (d) quinoline (**4**), (e) 1,2,4-oxadizole (**5**), (f) (*Z*)-(R$_1$amino)prop-2-en-1-ones (**6**), and (g) benzlyamides (**7**).

Table 2. Characterization of Selected Benzthiazoles from the qHTS[a]

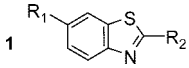

1

Analogue	R_1	R_2 (*N*-substituted)	IC_{50}	IC_{50Luc}	IC_{50PE}	$IC_{50Promega}$	$IC_{50SteadyGlo}$	$IC_{50BrightGlo}$	$IC_{50Renilla}$
a	Mesyl	thiophene-2-carboxamide	6.1 ± 1	1.1 ± 0.4	1.3 ± 1.1	9.5 ± 0.5	2.5 ± 1.3	3.2 ± 2.8	Inactive
b	Mesyl	5-methylthiophene-2-carboxamide	5.4 ± 0.05	1.1 ± 0.4	3.2 ± 0.4	Inactive	10 ± 5.8	13.3 ± 12.2	n.d.
c	Me	thiophene-2-carboxamide	1.4 ± 0.1	0.5 ± 0.1	1.7 ± 0.4	>50	6.9 ± 0.12	6.7 ± 4.6	Inactive
d	OEt	2-methylfuran-3-carboxamide	4.2 ± 1	0.65 ± 0.11	5.7 ± 1.1	3.8 ± 1.3	3.6 ± 0.6	4	Inactive
e	OMe	2-methylfuran-3-carboxamide	2.1 ± 0.5	1.2 ± 0.34	4.5 ± 0.7	3.6 ± 0.6	10.3 ± 6.5	5.9 ± 1.6	Inactive
f	OEt	3-(thiophen-2-yl)urea	1.45 ± 0.1	0.6 ± 0.3	2.1 ± 0.5	Inactive	12.0 ± 0.0	11.3 ± 6.6	Inactive
g	H	(4-phenoxy)-1-(4-methylpiperazin-1-yl) ethanone	0.9 ± 0.1	0.3 ± 0.1	0.4 ± 0	Inactive	1 ± 0.5	6.5 ± 2.1	22.5 ± 8
h	H	2-phthalazin-1(2*H*)-one	0.2 ± 0.02	0.3 ± 0.1	0.15 ± 0.06	5.1 ± 1.1	0.6 ± 0.4	0.7 ± 0.7	Inactive

[a] PubChem CIDs: (**1a**) 670282, (**1b**) 1225609, (**1c**) 739615, (**1d**) 887167 (**1e**) 1245272, (**1f**) 4101591, (**1g**) 2350207, and (**1h**) 727725. Activity of compounds was determined via measurement of luminescence in the indicated format. IC_{50}, activity in primary assay (Lonza); IC_{50Luc}, activity against purified *P. pyralis* luciferase; IC_{50PE}, activity measured by using EasyLite; $IC_{50Promega}$, activity measured by using Kinase-Glo; $IC_{50SteadyGlo}$, activity in luciferase reporter gene detection mix; $IC_{50BrightGlo}$, activity in luciferase reporter gene detection mix; $IC_{50Renilla}$, activity against *R. reniformis*. Potencies in μM. n.d., not determined. Data shown are mean ± SD for at least four replications.

ATP binding and the formation of the luciferly adenylate intermediate. Stable analogues of the luciferyl−AMP intermediate have been shown to be potent inhibitors of firefly luciferase that act in a noncompetitive manner.[23]

Quinoline Series. A series of substituted quinilones were examined on the basis of the known activity of quinolines as competitive inhibitors of ATP-dependent enzymes such as protein kinases.[24] Compounds containing core **4** contained fewer library analogues with potency in the micromolar range (Figure 4d). However, approximately half of the activity was associated with class 1 curves.

Representative compounds were obtained and subjected to the analysis described above (Table 3). In all cases, the inhibition mediated by these compounds could be competed by varying either luciferin or ATP, and the compounds were found to be inactive at 1 mM concentrations of both substrates (Figure 5b). As mentioned above, the absence of inhibition in the reporter gene formulations may be explained by the probable high substrate concentrations present in these assay mixtures and the dependence of potency on substrate concentration observed for the quinoline series. Further, none of the compounds showed strong inhibition in the *P. pennsylvanica* firefly reagent cocktail,

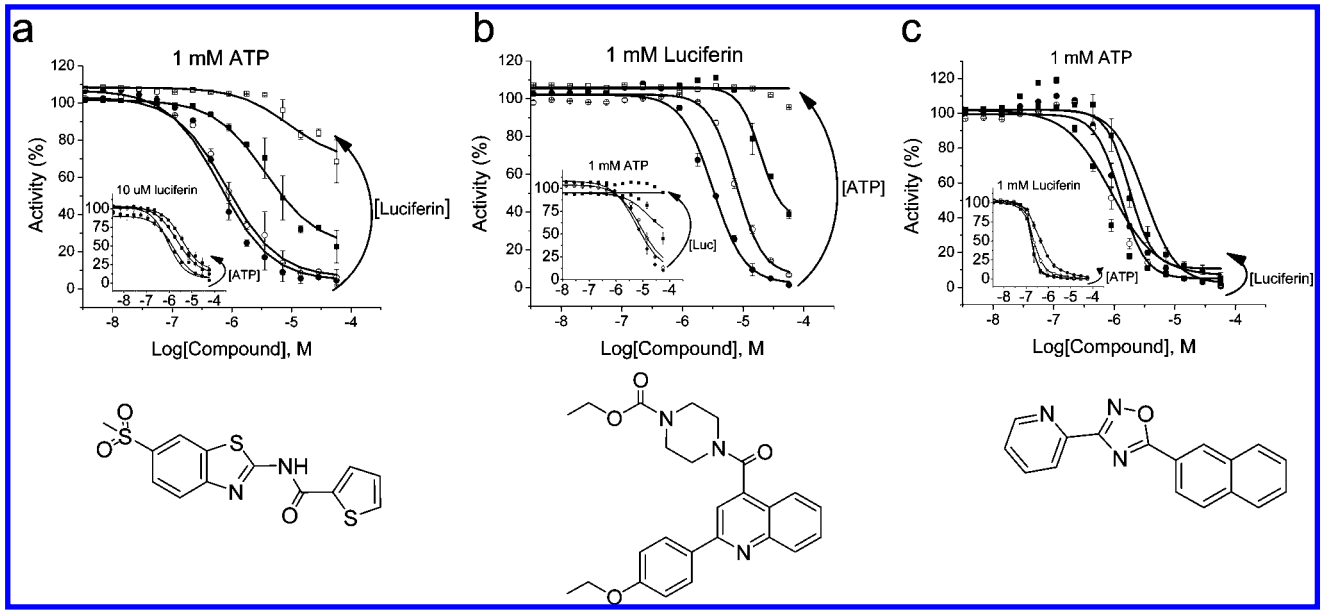

Figure 5. Dependence of inhibition on substrate concentration for three representative series. Luciferin or ATP was varied at (●) 1 μM, (○) 10 μM, (■) 100 μM, and (□) 1000 μM. (a) Substrate variation data for the benzthiazole (**1a**). The graph shows that inhibition can be relieved upon increasing the luciferin concentration, and the inset graph shows that ATP variation has little effect on the inhibition (holding the luciferin concentration constant at 10 μM, approximately the K_m). (b) Substrate variation data for the quinoline (**4e**). The graph shows that inhibition can be relieved when either the ATP or the luciferin concentration (inset graph) is increased. (c) Substrate variation data for the 1,2,4-oxadiazole (**5c**). The graph shows that the inhibition remains relatively constant when varying either the luciferin or the ATP concentration (inset graph).

Table 3. Characterization of Selected Quinoline Analogues from the qHTS[a]

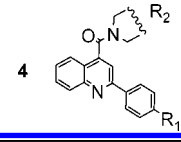

Analogue	R_1	R_2	IC_{50}	IC_{50Luc}	IC_{50PE}	$IC_{50Promega}$	$IC_{50SteadyGlo}$	$IC_{50BrightGlo}$	$IC_{50Renilla}$
a	OEt		1.4± 0.1	0.7± 0.5	1.0± 0.3	>50	Inactive	Inactive	11± 6
b	Me	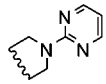	4.5± 0.8	4± 1.5	4.6± 1.3	>50	Inactive	Inactive	>25
c	OEt	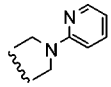	0.5± 0.02	0.4± 0.2	0.6± 0.2	>50	Inactive	Inactive	11± 6
d	OEt		2.4± 0.2	1.3 ± 0.7	1.1± 0.2	>50	Inactive	Inactive	>25
e	OEt	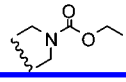	1.4± 0.3	0.9± 0.4	1.0± 0.3	>50	Inactive	Inactive	20± 10

[a] PubChem CIDs: (**4a**) 3241312, (**4b**) 2093195, (**4c**) 3238892, (**4d**) 1540951, and (**4e**) 3237815. Activity of compounds was determined via measurement of luminescence in the indicated format. IC_{50}, activity in primary assay (PK-Light); IC_{50Luc} activity against purified *P. pyralis* luciferase; IC_{50PE}, activity measured by using EasyLite; $IC_{50Promega}$, activity measured by using Kinase-Glo; $IC_{50SteadyGlo}$, activity in luciferase reporter gene; $IC_{50BrightGlo}$, activity in luciferase reporter gene detection mix; $IC_{50Renilla}$, activity against *R. reniformis*. Potencies in μM. Data shown are mean ± SD for at least four replications.

suggesting that these compounds do not interact with a conserved site in the two luciferases.

The quinoline series was also the only series analyzed that showed consistent inhibition against the *R. reniformis* luciferase. In general, this inhibition was ~10-fold weaker than what was found against purified *P. pyralis*, but some compounds showed $IC_{50} \approx 10$ μM (e.g., **4a**, CID 3241312 and **4c**, CID: 3238892), which is comparable to typical compound screening concentrations. Light attenuation is not the likely mechanism of *R. reniformis* inhibition by these series (see below). It is possible that the 2-phenylquinoline core is also able to antagonize *R. reniformis* substrate binding by mimicking the phenyl-imidazopyrazinone core of coelenterazine (see Figure 1). Substitutions at all three phenyl groups around the imidazopyrazinone core have been used to modulate the wavelength of bioluminescence of *R. reniformis* luciferase, suggesting some plasticity in substrate binding.[25]

Luciferase Inhibitors Showing Noncompetitive Inhibition. We noted several compound series for which the observed inhibition had marginal dependence on the concentration of

Table 4. Characterization of Selected 1,2,4-Oxadiazoles from the qHTS[a]

5 

Analogue	R_1	R_2	IC_{50}	IC_{50Luc}	IC_{50PE}	$IC_{50Promega}$	$IC_{50SteadyGlo}$	$IC_{50BrightGlo}$	$IC_{50Renilla}$
a	phenyl	naphthalen-2-yl	1.6 ± 0.0	0.4 ± 0.1	2.1 ± 0.4	Inactive	1.4 ± 0.4	2.6 ± 2.1	Inactive
b	pyridin-2-yl	3-chlorophenyl	2.1 ± 0.4	0.5 ± 0.2	0.7 ± 0.1	7.4 ± 1.4	1.5 ± 0.1	1.2 ± 0.9	>50
c	pyridin-2-yl	naphthalen-2-yl	0.22 ± 0.04	0.1 ± 0.03	0.22 ± 0.04	11.3 ± 1.8	0.2 ± 0.1	0.2 ± 0.1	25 ± 7.9
d	phenyl	2,4-dimethoxyphenyl	0.4 ± 0.06	0.15 ± 0.06	1.1 ± 0.2	13 ± 0.0	1.1 ± 0.2	0.3 ± 0.05	Inactive
e	pyridin-2-yl	3-chloro-4-methylphenyl	2.1 ± 0.2	0.22 ± 0.04	0.8 ± 0.1	22 ± 2.1	1.6 ± 0.3	1.4 ± 1.1	Inactive
f	pyridin-2-yl	3,4-dichlorophenyl	4.1 ± 0.5	0.84 ± 0.4	1.9 ± 0.3	19 ± 1.4	3.3 ± 1.3	3.9 ± 2.8	Inactive
g	4-methylphenyl	2-bromophenyl	3.3 ± 0.5	1.0 ± 0.9	2.3 ± 0.5	Inactive	11 ± 3.2	12 ± 7.9	Inactive
h	pyridin-2-yl	5-bromofuran-2-yl	13 ± 1.0	3.2 ± 1.4	5.1 ± 0.5	12 ± 5.5	2.6 ± 0.75	12 ± 1.9	Inactive
i	pyridin-2-yl	bipheny-4-yll	2.6 ± 1.9	0.1 ± 0.03	0.5 ± 0.1	Inactive	0.14 ± 0.09	0.3 ± 0.2	Inactive
j	phenyl	2-chloro-4-methylphenyl	0.5 ± 0.03	0.15 ± 0.2	0.4 ± 0.1	10.5 ± 2.2	0.16 ± 0.05	0.3 ± 0.2	Inactive

[a] PubChem CIDs: (**5a**) 3241690, (**5b**) 650707, (**5c**) 926663, (**5d**) 893238, (**5e**) 660258, (**5f**) 695758, (**5g**) 867101, (**5h**) 752709, (**5i**) 838877, and (**5j**) 2056784. Activity of compounds was determined via measurement of luminescence in the indicated format. IC_{50}, activity in primary assay (PK-Light); IC_{50Luc}, activity against purified *P. pyralis* luciferase; IC_{50PE}, activity measured by using EasyLite; $IC_{50Promega}$, activity measured by using Kinase-Glo; $IC_{50SteadyGlo}$, activity in luciferase reporter gene detection mix; $IC_{50BrightGlo}$, activity in luciferase reporter gene detection mix; $IC_{50Renilla}$, activity against *R. reniformis*. Potencies in μM. Data shown are mean ± SD for at least four replications.

Table 5. Characterization of Selected (*Z*)-(R_1amino)prop-2-en-1-ones from the qHTS

6 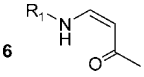

Analogue	R_1	R_2	IC_{50}	IC_{50Luc}	IC_{50PE}	$IC_{50Promega}$	$IC_{50SteadyGlo}$	$IC_{50BrightGlo}$	$IC_{50Renilla}$
a	3-fluorophenyl	benzo[*d*][1,3]dioxol-5-yl	1.2 ± 0.2	0.3 ± 0.1	1.2 ± 0.2	>50	0.9 ± 1.1	1.9 ± 1.7	Inactive
b	pyridin-2-yl	4-chlorophenyl	4.1 ± 0.8	2.0 ± 1.1	4.7 ± 1.0	Inactive	0.5 ± 0.2	1.2 ± 0.8	Inactive
c	2-bromophenyl	pyridin-2-yl	0.17 ± 0.04	0.08 ± 0.07	0.17	10 ± 0.07	0.2 ± 0.1	0.08 ± 0.02	>50
d	4-fluorophenyl	furan-2-yl	3.6 ± 0.6	1 ± 0.5	1.1 ± 0.18	14.2 ± 2.3	4 ± 0.6	3.6 ± 0.6	Inactive
e	4-dimethylaminophenyl	phenyl	0.6 ± 0.1	0.21 ± 0.05	0.4 ± 0.1	3.2 ± 1.4	0.6 ± 0.4	0.7 ± 0.7	11

[a] PubChem CIDs: (**6a**) 5310801, (**6b**) 5310655, (**6c**) 2260658, (**6d**) 2195987, and (**6e**) 2188632. Activity of compounds was determined via measurement of luminescence in the indicated format. IC_{50}, activity in primary assay (PK-Light); IC_{50Luc}, activity against purified *P. pyralis* luciferase; IC_{50PE}, activity measured by using EasyLite; $IC_{50Promega}$, activity measured by using Kinase-Glo; $IC_{50SteadyGlo}$, activity in luciferase reporter gene detection mix; $IC_{50BrightGlo}$, activity in luciferase reporter gene detection mix; $IC_{50Renilla}$, activity against *R. reniformis*. Potencies in μM. Data shown are mean ± SD for at least four replications.

either substrate, which is consistent with a noncompetitive inhibition mode (i.e., $IC_{50} \approx K_i$).[26] One of the most prominent series in this category identified in the qHTS were compounds containing core **5** (1,2,4-oxadiazole, Table 4). Here, among the large number of analogues present within the compound library, approximately one-third were active (Figure 4e), displaying a broader range of potencies than the benzoxazole series (Figure 4c).

Varying substrate concentration did not significantly change the IC_{50} values of the oxadiazole series (Figure 5c). Compounds in this series showed inhibition across all the luciferase cocktails containing *P. pyralis*, with weaker inhibition at the *P. pennsylvanica* firefly reagent cocktail (Table 4). The most potent oxadiazole **5c** (CID 926663, Table 4, $IC_{50} \approx 200$ nM) inhibited all detection reagents but only weakly inhibited the *P. pennsylvanica* and *R. reniformis* luciferases. In compound **5c**, a pyridine at position R_1 improves the potency of this series between 4- and 10-fold over phenyl (compound **5a**, CID 3241690).

Another series contained core **6** ((*Z*)-(R_1amino)prop-2-en-1-one). Although few closely related analogues were present in the compound collection for this series, nearly half of the actives showed class 1 concentration−response curves, and several showed potencies well below 1 μM (Figure 4f). Representative analogues containing core **6** were obtained (compounds **6a**−**e**, Table 5) and subjected to further analysis. Compound **6c** (CID 2260658) was one of the most potent compounds identified within this series ($IC_{50} \approx 100$ nM). Variation of both ATP and luciferin showed inhibition of a noncompetitive nature similar to the oxadiazole shown in Figure 5c.

A series of compounds containing core **7** (benzyl amides, Table 6) also contained noncompetitive inhibitors with numerous analogues, among which nearly one-third were active in the luciferase assay (Figure 4g). Several of these compounds showed activity <1 μM, with an average potency of just below 10 μM. The most potent compound **7c** (CID 649849), carrying a 5-methyl pyridin-2-yl at position R_1, had an IC_{50} of ~300 nM in all luciferase detection reagents except the *P. pennsylvanica* firefly reagent cocktail. This series was largely inactive on *R. reniformis* luciferase, which is in agreement with the other noncompetitive series. The apparent *R. reniformis* luciferase activity of compound **7a** (CID 5483116) is thought to derive from luminescence attenuation not enzyme inhibition (discussed further below). Compound **7a** is a known γ-aminobutyric acid receptor antagonist. We noted several additional compounds, the biological activities of which are known, and we describe these in the following section.

Luciferase Activity within Known Bioactive Compounds. The libraries screened in this study included a number of commonly used bioactive compound libraries and some purified natural product libraries obtained from commercial sources. We have indicated in Tables 7 and 8 the known bioactive compounds that were subjected to further analysis, and these are discussed in turn.

A series of bioactives including flavonoids and known inhibitors of enzymes such as kinases[27–29] is shown in Table 7. Many protein kinase HTS assays monitor ATP depletion through a reduction of luminescence from the ATP-dependent firefly luciferase reaction. Here, compounds that inhibit both the luciferase and the protein kinase will have opposite effects on the luminescent signal, potentially resulting in false negatives. In general, these compounds were of low molecular weight (MW) (<300). Similar to series with cores **1**−**7** described above, the compounds had greatly reduced or no activity against *P.*

Table 6. Characterization of Selected Benzylamides from the qHTS[a]

7

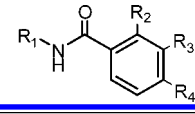

Analogue	R_1	R_2	R_3	R_4	IC_{50}	IC_{50Luc}	IC_{50PE}	$IC_{50Promega}$	$IC_{50SteadyGlo}$	$IC_{50BrightGlo}$	$IC_{50Renilla}$
a	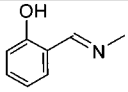	OH	H	H	2.5	0.8± 0.6	3.6± 0.6	Inactive	20	2.6	20± 6.5
b	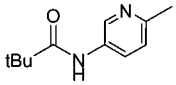	H	OH	H	5	0.7± 0.8	0.8± 0.3	>30	0.8± 0.9	7.2± 3.5	Inactive
c	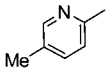	OMe	H	OMe	0.25± 0.15	0.08± 0.07	0.28± 0.05	14.2± 2.3	0.5± 0.1	0.2± 0.03	Inactive
d	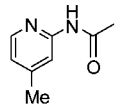	H	H	OMe	0.98± 0.04	0.41 ± 0.14	0.37 ± 0.10	6.9 ± 0.42	1.2± 0.07	1.0± 0.7	Inactive
e	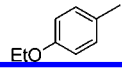	OMe	H	H	2.8± 0.6	0.6± 0.3	1.5± 0.4	Inactive	>50	8.3± 0.0	Inactive

[a] PubChem CIDs: (**7a**) 5483116 (Tocris-2143), (**7b**) 653989, (**7c**) 649849, (**7d**) 1540545, and (**7e**) 94777. Activity of compounds was determined via measurement of luminescence in the indicated format. IC_{50}, activity in primary assay (PK-Light); IC_{50Luc}, activity against purified *P. pyralis* luciferase; IC_{50PE}, activity measured by using EasyLite; $IC_{50Promega}$, activity measured by using Kinase-Glo; $IC_{50SteadyGlo}$, activity in luciferase reporter gene detection mix; $IC_{50BrightGlo}$, activity in luciferase reporter gene detection mix; $IC_{50Renilla}$, activity against *R. reniformis.* Potencies in μM. Data shown are mean ± SD for at least four replications.

pennsylvanica and *R. reniformis*. The most potent compound against *P. pyralis* luciferase was flavonoid **9** from the TimTec library, having an IC_{50} of 50 nM against purified firefly luciferase, demonstrating noncompetitive behavior and activity in the firefly-based luminescence reporter assays (see p53 assay, PubChem AID 902 and 924). However, another flavonoid, **10**, annotated as a noncompetitive inhibitor of mitogen activated protein kinase,[30] showed significantly weaker inhibition that was relieved by using 1 mM concentrations of luciferin or ATP. Inhibition by compound **8** (indoprofen)[31] and compound **12** could also be reduced by using high concentrations of either substrate, whereas compound **11** (pifithrin-α),[28] containing an imino-tetrahydrobenzothiazole core, exhibited noncompetitive inhibition; the potency did not vary appreciably in the presence of 1 mM of each substrate (IC_{50} = 1.6 μM).

In addition to the previously described resveratrol,[10] we observed a series of diaryl compounds, the predominant structural class of which is associated with inhibition of metabotropic glutamate signaling (Table 8). Inhibition by all these compounds was relieved in the presence of 1 mM luciferin and ATP, and the majority showed reduced inhibition against *R. reniformis*. The exceptions were inhibitors **15** and **16**, involved with glutamate pharmacology;[32,33] however, these compounds demonstrated optical interference (see below, Supporting Information, Figure S1).

Potential Binding Modes of the Quinoline and Benzthiazole Inhibitors. The substrate-competitive binding mechanism of the benzthiazole and quinoline series supported modeling these into the active site of firefly luciferase. The quinoline core is a known scaffold for many ATP-competitive protein kinase inhibitors, and as mentioned above, compounds with dual luciferase and protein kinase activity could result in false negatives when firefly luciferase-based detection is used. Therefore, we were interested in comparing the adenosine pockets of protein kinases and firefly luciferase to examine whether this quinoline series could be accommodated by the ATP binding pocket of protein kinases. Also, to examine the mode of binding of the benzthiazole series, we modeled this into the active site of firefly luciferase.

We first examined the adenosine binding pockets for both firefly luciferase and a typical protein kinase, the EGFR kinase. In both the luciferase and the EGFR kinase cases, adenosine binds in a narrow groove but with quite different contacts (Figure 6a,c). The packing contacts in protein kinases, Val702, Ala719, and Leu820 (Figure 6a), involve lipophilic amino acids, typically Val, Ala, Leu, or Met. In contrast, the stacking interactions between adenosine and luciferase include an edge−face aromatic interaction (Tyr342) and packing between the backbone of the β-turn between Gly318 and Pro320. In both cases, adenosine further interacts through hydrogen bonds with its N1 and amino group. The hydrogen bonds to the protein kinase are to a backbone NH and a carbonyl oxygen of a short β-strand called the hinge region. In the case shown, the hydrogen bonds are with the NH of Met769 and the backbone carbonyl of residue 767. For the luciferase protein, the NH2 of adenosine forms a hydrogen bond with the backbone carbonyl of Gly341, whereas N1 of adenosine forms a water-mediated hydrogen bond with the side chain of Gln340. In both cases, the ribose makes limited contacts with the respective binding site and appears to act more as a spacer between adenosine and the phosphates. The 2′-hydroxyl interacts with Asp424 of the Japanese firefly luciferase. In many protein kinases, an interaction between the 2′-hydroxyl and an aspartic acid is also observed. This aspartic acid is the equivalent to Cys773 in EGFR shown in Figure 6a, whereas in other protein kinases, this residue can be Asp, Glu, Gln, Ser, Thr, and Ala, which indicates that this is not a critical interaction. Finally, the motifs for recognizing the phosphates bear no similarity between the two enzymes. The phosphates of ATP interact with the protein kinase through a pair of bound Mg^{2+} ions. Additionally, the protein kinase provides a lysine (Lys721 in EGFR) to interact with the α-phosphate. The lysines are the only point of similarity between the protein kinase and

Table 7. Known Enyzme-Based Inhibitors from the qHTS[a]

#	Structure	Common Name	IC_{50}	IC_{50Luc}	IC_{50PE}	$IC_{50Promega}$	$IC_{50SteadyGlo}$	$IC_{50BrightGlo}$	$IC_{50Renilla}$
8	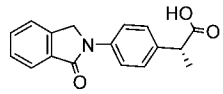	Indoprofen	4.7	0.2± 0.1	3.6	>50	10	5.3	n.d.
9	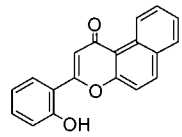	Flavanoid	0.7	0.05± 0.03	0.2	14	0.06	0.09	Inactive
10	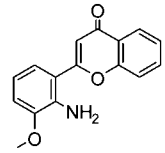	PD98059	6.4	6.2± 0.6	11	Inactive	>100	60	Inactive
11	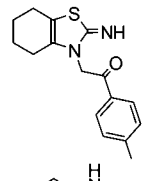	Pifithrin−α	1.1± 0.18	0.32± 0.07	1.8± 0.29	Inactive	2.8± 0.5	0.6± 0.09	Inactive
12	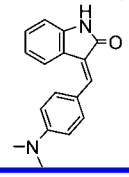	SU4312	2.5± 0.0	0.8± 0.2	4.5± 0.7	Inactive	14.2± 2.3	10	19± 11

[a] Activity of compounds was determined via measurement of luminescence in the indicated format. IC_{50}, activity in primary assay (PK-Light); IC_{50Luc} activity against purif ied *P. pyralis* luciferase; IC_{50PE}, activity measured by using EasyLite; $IC_{50Promega}$, activity measured by using Kinase-Glo; $IC_{50SteadyGlo}$, activity in lucif erase reporter gene detection mix; $IC_{50BrightGlo}$, activity in luciferase reporter gene detection mix; $IC_{50Renilla}$, activity against *R. reniformis*. Potencies in μM. n.d., not determined. Data shown are mean ± SD for at least four replications.

luciferase phosphate-binding sites (Lys721 in EGFR and Lys531 in luciferase). The phosphate of AMP interacts with luciferase through a large number of backbone and side-chain hydrogen bonds.

We next modeled the quionline **4c** (CID 3238892) into the adenosine pocket of luciferase. The quinoline/quinazoline core is a well-known scaffold for protein kinases and represents one of the earliest classes of small-molecule protein kinase inhibitors.[34] It has been shown crystallographically that the quinazoline/quinoline binds to the protein kinase through a key hydrogen bond with N1 to the hinge backbone NH of the protein kinase;[17] in essence, N1 of the quinoline mimics the interaction between adenosine N1−Met769 NH (Figure 6b). In this binding mode, however, the protein kinase adenosine pocket would not stericly tolerate a phenyl ring at the C2 position for the quinoline-based luciferase inhibitor because of a steric clash with the backbone carbonyl of residue 767 (Figure 6b). Indeed, in order to accommodate the 2-phenyl substitution, the crystallographically observed binding mode for the quinazoline would have to shift so far that the N1 nitrogen would no longer be able to form the critical interaction with the backbone NH of the hinge. Compound **4c** could be accommodated in the luciferase active site in a mode where both the AMP and luciferin binding would be expected to be affected, which is consistent with the substrate variation studies mentioned above (see Figure 6d). This points the 2-phenyl toward the luciferin-binding site and the piperazine and subsequent polar groups toward the phosphate-binding site which is both polar and solvent-exposed; this is consistent with the tolerance for a wide variety of polar substituents. Thus, these larger (MW > 375) quinoline-based luciferase inhibitors can be accommodated into the luciferase substrate pocket but are unlikely to bind to protein kinases with the binding mode consistently observed in protein kinase/quinoline cocrystal structures. (Both **4d** (CID 1540951) and **4c** were subsequently checked for activity against the kinases IR, LCK, EGFR, and PKA and were found to be inactive (the highest tested concentration was 20 μM; Reaction Biology Corp., Malvern, PA).)

Modeling of the benzthiazole-based luciferase inhibitor **1a** into the luciferase pocket illustrates how this molecule can fit into the narrow pocket occupied by that of oxyluciferin (Figure 6e,f). This pocket is formed from above by aromatic stacking with Phe249 and from below by the C_β of Ala350 and the backbone of Gly343−Leu344. This orientation points the thiophene toward the AMP pocket, where extension at the R_2 position would protrude into the AMP phosphate-binding site and would suggest a more mixed inhibition pattern for larger R_2 substituents, which is consistent with what was observed with compounds **1g** and **1h**.

Examination of Light Attenuation by Luciferase Inhibitors. A mode of nonspecific inhibition could arise through compound-specific absorbance or light scattering. In this case, compounds that interfere with luminescence detection could appear as luciferase inhibitors. We compared the absorbance spectrum for representative compounds from each series to the emission spectrum of either firefly or *R. reniformis* luciferase

Table 8. Known Biological Actives from the qHTS[a]

	#	Structure	Common Name	Annotation	IC_{50}	IC_{50Luc}	IC_{50PE}	$IC_{50Promega}$	$IC_{50SteadyGlo}$	$IC_{50BrightGlo}$	$IC_{50Renilla}$
R= 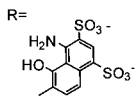	**13**	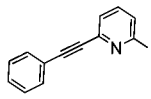	MPEP	GluR	6.6	4.7± 0.5	7.4	Inactive	>100	30	Inactive
	14	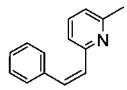	SIB1893	GluR	17	4.3± 0.8	11	>50	>100	24	Inactive
	15	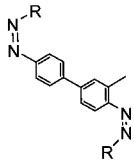	Evans Blue	Glutamate uptake	6.9	1.7	7.6	20	22	17	10
	16	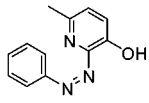	SIB1757	GluR	1.7± 0.8	4.5± 0.7	1.26± 0.0	1.8± 0.3	1.6	2	36± 5.8
	17	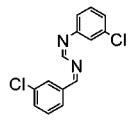	DCB	GluR	7.8± 5.5	4.5±0.7	11.4±7.4	Inactive	Inactive	Inactive	>50
	7a	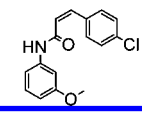	SCS	GABA	2.5± 0.0	0.8± 0.6	3.6± 0.6	Inactive	20	12.6	20± 6.5

[a] Activity of compounds was determined via measurement of luminescence in the indicated format. IC_{50}, activity in primary assay (PK-Light); IC_{50Luc} activity against purif ied *P. pyralis* luciferase; IC_{50PE}, activity measured by using EasyLite; $IC_{50Promega}$, activity measured by using Kinase-Glo; $IC_{50SteadyGlo}$, activity in lucif erase reporter gene detection mix; $IC_{50BrightGlo}$, activity in luciferase reporter gene detection mix; $IC_{50Renilla}$, activity against *R. reniformis*. Potencies in μM. Data shown are mean ± SD for at least four replications.

(Figure 7a). The majority of the compounds characterized here were colorless in solution and absorbed light below 400 nm. However, a few compounds absorbed light between 400 and 550 nm. To test light attenuation, we prepared samples in a split cuvette; one-half of the cuvette was filled with the luciferase reaction and the other half contained the compound solution in the same buffer. In this experiment, measurement of luminescence through the compound solution gives information on absorbance, and the same cuvette can be used to measure unattenuated luminescence by simply rotating the cuvette so that the light is detected directly from the luciferase reaction. We selected this mode of detection because we wanted to measure optical interferences by these compounds in a manner that was completely separate from any enzyme-specific effects. The most highly colored compound tested in follow-up assays was compound **15**, a dark blue dye (showing broad absorption between 450 and 600 nm, data not shown) that weakly inhibited both *R. reniformis* and the reporter gene formulations (10−20 μM IC_{50}), and we found that this compound was able to quench approximately 50% of the luminescence from either *R. reniformis* or *P. pyralis* luciferases at a concentration of 20 μM (Supporting Information, Figure S1). Similarly, compounds such as lissamine or napthol blue black that showed either pink or dark blue solutions, respectively, were able to attenuate luminescence produced by *P. pyralis* luciferase, whereas compounds having yellow or brown solutions such as tartrazine or for compound **16** did not affect *P. pyralis* luciferase luminescence, even at 100 μM; this is consistent with the emission spectrum of firefly luciferase. However, when *R. reniformis* luciferase was used in the reaction, we were able to detect light attenuation at 100 μM compound **16** (Supporting Information, Figure S1), which is consistent with its visible absorbance spectrum (absorption between 400 and 500 nm, Figure 7a). Also, an active series of 3-substituted 2*H*-chromen-2-ones contained a potent member **18** (CID 94381, Supporting Information, Figure S1, Figure 7b), and we observed a fluorescent-yellow solution for this compound with strong absorption between 400 and 525 nm (Figure 7a). The absorbance of compound **18** largely overlapped the emission spectrum of *R. reniformis* luciferase (Figure 7a), and we found that compound **18** attenuated light emitted from *R. reniformis* but not *P. pyralis* luciferase (Figure 7c).

Discussion

Luciferase enzymes are used widely in HTS as reporters in cell-based assays and as sensors of ATP concentration in cell viability or in biochemical assays of kinases; their use has been extended to measure the activity of proteases and cytochrome P450s as well.[3] Because of this widespread use, an understanding of the chemotypes that can directly affect this enzyme's activity and thus lead to assay-related artifacts is critical. In addition, on the basis of the evolutionary diversity of firefly luciferases, their utilization of ATP, and the fact that these enzymes are naturally outfitted with a robust assay, luciferases are an ideal model system for chemical genomics. We have therefore tested the activity of a large publicly available chemical library against firefly luciferase and established a comprehensive profile of the library members that inhibit the enzyme.

The assay showed excellent performance in a continuous robotic experiment where concentration−response curves for 72 377 compounds were determined in a single experiment.

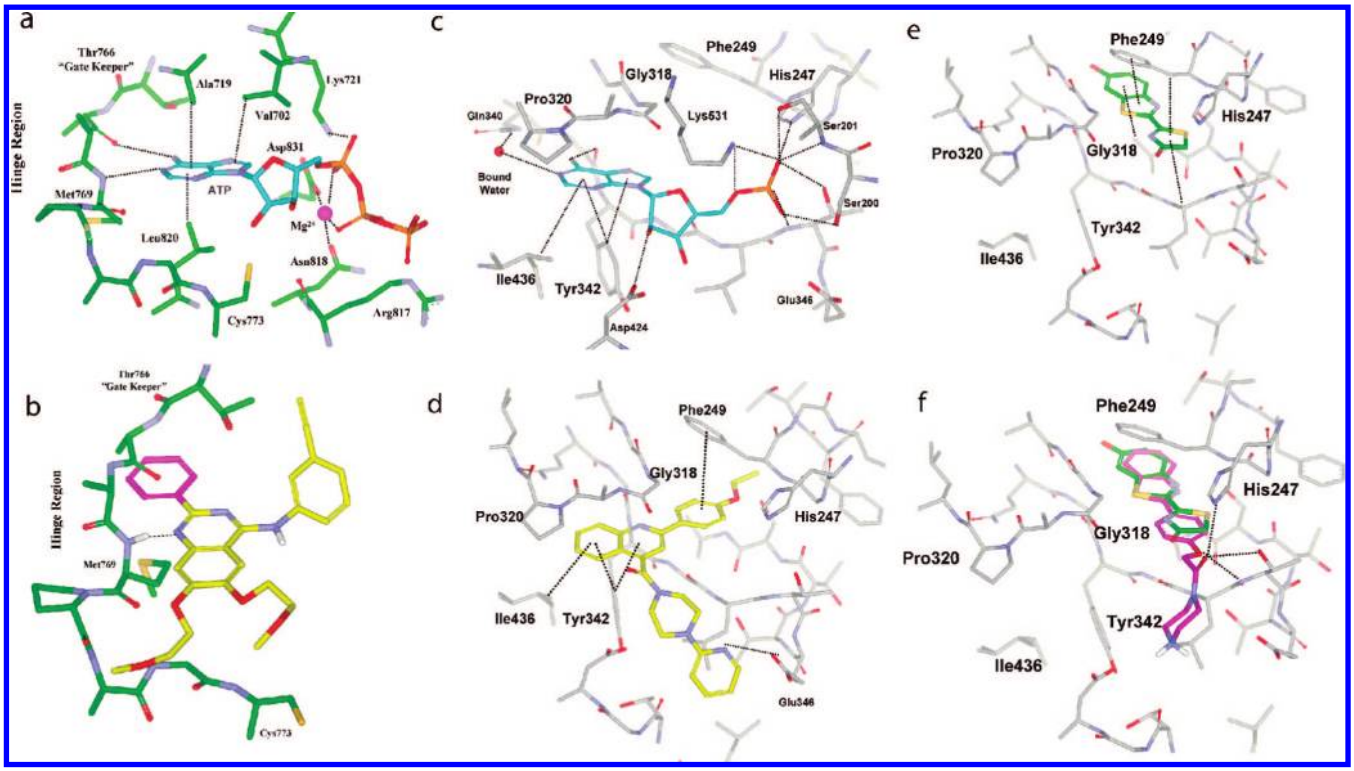

Figure 6. Modeling of substrate-competitive inhibitors. The EGFR protein kinase chain (green chains, a and b) and the Japanese firefly luciferase (gray chains, c−f) in complexes with adenosine (ATP or AMP) or as models of the putative inhibitor complexes. (a) The EGFR receptor kinase adenosine pocket shown with Mg−ATP bound taken from the EGFR cocrystal structure (PDB code 2GS7). (b) Modeling of 2-phenyl substituted quinazoline/quinolines. The binding mode of a quinazoline-based kinase inhibitor (yellow chain) in the EGFR adenosine pocket. The portion shown in yellow was taken from the EGFR cocrystal structure 1M17. The 2-phenyl (purple) substituent was added with ideal geometry, keeping the rest of the molecule fixed and ignoring the protein. In this binding mode, the N1 of the quinazoline makes the equivalent hydrogen bond to N1 of the adenosine. A phenyl at the position 2 of the quinazoline (purple side chain) directly clashes with the backbone of the hinge residues, in this case 767. In order to sterically fit, the 2-phenyl quinazoline would have to considerably shift position, significantly disrupting the critical N1-hinge−NH hydrogen bond. (c) Binding of AMP in firefly luciferase taken from the cocrystal structure (PDB code 2D1R). (d) Modeling of the quinoline **4c** (yellow chain) into the luciferase pocket. The best fit has the quinoline occupying approximately the same space as the purine of AMP, and N1 of the quinoline is near N7 of the purine. This allows the 2-phenyl substituent to reach into the luciferin binding pocket in nearly the identical space as shown for the benzthiazole. This quinoline-series binding mode further allows the polar substituent to extend into the phosphate-binding region, which is consistent with the fact that the luciferase inhibitory activity is tolerant of a number of polar substituents at this position. (e) Binding of luciferin in firefly luciferase taken from the cocrystal structure (PDB code 2D1R). (f) Modeling of the benzthiazole **1a** (purple chain) into the luciferase pocket. The structure is shown to occupy nearly identical space as the luciferin (green overlaid structure), with the substitution at the four positions of the phenyl ring reaching into the phosphate binding region of AMP.

With this primary screening data, we performed SAR analyses to identify structural characteristics of the inhibitors. The active series identified in the luciferase qHTS provide a rich database for comparison to other screening results obtained from commonly used firefly luciferase-based detection reagents (PubChem AID 411; we will continue to update this data set as new compounds are added). All of the identified chemical series also inhibited wild-type *P. pyralis* luciferase, and many inhibited luciferase-based detection reagents from other suppliers. The potencies of these compounds were within the concentration ranges typically were tested in HTS (e.g., 10 μM), many compounds showed IC_{50} values <1 μM. Additionally, comparison of the luciferase actives to 39 other qHTS campaigns performed at our center indicated that these compounds exhibited activity in assays utilizing luciferase, including one that employs a luciferase from the luminous click beetle *P. plagiophthalamus*. Therefore, these scaffolds will be useful to flag, because these compounds have the potential of inhibiting this common reporter in a variety of HTS formats. We noted that a reporter-gene-based assay that used Steadylite (Perkin-Elmer reagent; PubChem AID 618) for detection showed a 53% overlap between the actives derived by using a 6 SD cutoff of the reported percent control values and our luciferase actives showing class 1 curves. In addition, for compounds identified as activators in cell-based luciferase reporter assays (e.g., AID 522), we noted an enrichment (>10-fold) of luciferase inhibitors suggesting the potential of reporter stabilization through luciferase-inhibitor complex formation.

The most prominent clusters identified in our study contained the benzthiazole, benzimidazole, or benzoxazole core. The high representation of these chemotypes in luciferase actives is likely related to the benzthiazole-based luciferin substrate and ATP dependence of firefly luciferase. Several of the benzthiazole series were competitive with luciferin; however, modulation of the R_2 group could change the substrate dependence to a noncompetitive mode, potentially by engaging the adenylate-binding site as suggested by our modeling studies (Figure 6).

One of the most striking practical and evolutionary features of nearly all the luciferase actives identified here was their relative inactivity against the luciferase detection reagent that uses a variant of *P. pennsylvanica* firefly luciferase. Although certain compounds showed appreciable inhibition ($IC_{50} \leq 10$ μM), the majority was inactive, and none showed inhibition comparable to what was observed in *P. pyralis*-based reagents.

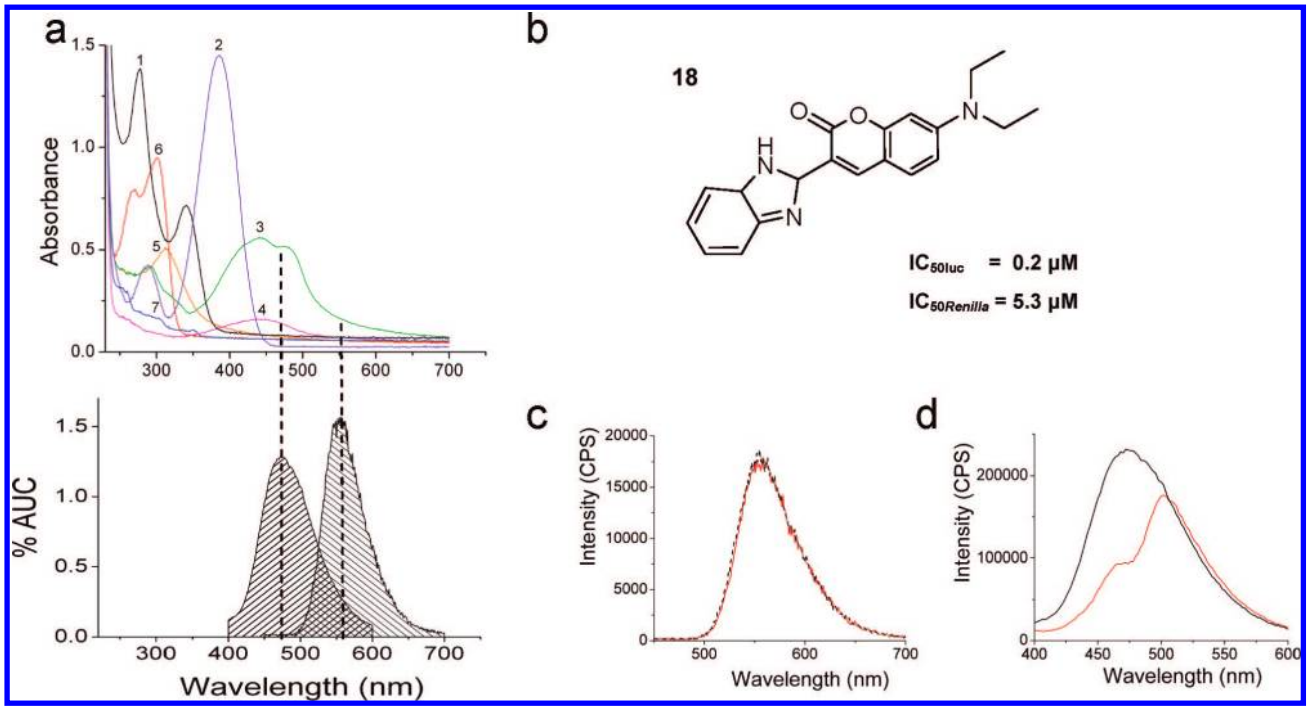

Figure 7. Evaluation of light attenuation by luciferase inhibitors. (a) Top absorbance spectra are shown for quinolione **4a** (1, black), (*Z*)-(*R*$_1$amino)prop-2-en-1-one **6a** (2, purple), coumarin **20** (3, green), mGluR5 antagonist **16** (4, magenta), benzthiazole **1d** (5, orange), benzylamide **7a** (6, red), and oxadizaole **5c** (7, blue). Lower graph on left shows the luminescence spectra of *R. reniformis* luciferase (left spectrum) vs firefly luciferase (right spectrum). Emission spectra are shown as percentages of the AUC for each spectrum. Dotted lines correspond to the emission maxima. (b) Structure of coumarin **18** and potencies for firefly and *R. reniformis* luciferases. (c) Firely luminescence in the absence (black line) and presence (red line) of 100 μM compound **18**. (d) *R. reniformis* luminescence in the absence (black line) and presence (red line) of 100 μM compound **18**.

However, small changes in structure within a benzthiazole scaffold (compare compounds **1a** and **1b**) could lead to weak inhibition, suggesting that inhibition of *P. pennsylvanica* is just as achievable as what we observed here for *P. pyralis* but will exhibit a different SAR. We are currently testing this by using a reagent cocktail containing *P. pennsylvanica* luciferase and a full qHTS of the compound collection to determine the extent of inhibition.

Compounds such as **18** illustrate the complexity of deconvoluting nonspecific interference by light absorption from genuine inhibition of the luciferase enzyme. Compound **18** showed potent inhibition in detection reagents employing firefly luciferase, and this inhibition could be relieved by adding excess substrates. Furthermore, the benzimidazole core present in compound **18** is consistent with the SAR shown here for firefly luciferase inhibitors, and closely related analogues were present in the luciferase screen that showed greatly reduced activity (e.g., compound **20**, CID 100335, Supporting Information, Table S1). Therefore, this series appears to be a genuine inhibitor of the firefly luciferase enzyme. However, this series also contains a coumarin chromophore, and we observed a potency of 5 μM for compound **18** against *R. reniformis* luciferase. From the light-attenuation experiment and the absorbance spectrum of this compound, it is possible that its apparent luciferase-inhibition activity is due to light absorption by the compound. It is difficult to correlate the amount of light attenuation observed in the cuvette experiment described above to that which occurs in a 1536-well assay volume. Therefore, although the coumarin series compounds exemplified by **18** appear to be firefly luciferase enzyme inhibitors, proper assignment of the activity against *R. reniformis* luciferase will require further investigation. In general, the interpretation problems presented by these types of colored compounds in HTS must be kept in mind, because they may act as enzyme inhibitors, light attenuators (particularly of blue-shifted luminescence), or both.

Several general strategies for determining and reducing luciferase assay interference can be derived from this profiling study. First, firefly or red-shifted variants of the *P. plagiophthalamus* luciferase should be employed whenever possible to eliminate nonspecific light attenuation effects. *R. reniformis* luciferase emits predominately blue luminescence (<3% of photons having wavelengths >600 nm),[35] rendering this luciferase more sensitive to optical interference by the many small-molecule compounds that absorb light in this range. A recent fluorescence profile of the library used here showed that ~0.1% of the compounds emitted fluorescence by using 480 nm excitation light[20] that is near the emission maximum of *R. reniformis*. Second, the use of bandpass filters to collect only the bathochromic light emitted by firefly luciferase (i.e., 600 nm) rather than the clear filters typically used is advisable in order to decrease light attenuation, if the signal strength is adequate. The use of bandpass filters in two-color dual-luciferase-based assays has been described for 1536-well cell-based assay systems,[36] and in principle, such a strategy could be used for any luminescent-based assay. This strategy is analogous to the use of red-shifted fluorophores to reduce compound fluorescence.[20] Third, the complete lack of luciferase activators identified in the present study suggests that luciferase-coupled reactions are ideal for assays where stimulation of the luminescent signal is desired, because the direct activation of the luciferase enzyme reaction by library compounds appears to be very rare.

The luciferases *P. pyralis* and *R. reniformis* have been a popular choice for constructing dual-luciferase-based assays, but the marked differences in SAR and optical interference we have observed here between these two luciferases suggest that such

assays should be constructed with more homologous pairs of luciferases. For example, red- and green-emitting versions of luminous click beetle *P. plagiophthalamus* luciferase have been engineered by introducing single amino acid changes in the luciferin-binding site.[37] In this assay format, a single detection reagent containing the benzthiazole-based luciferin substrate is added to detect both red- and green-emitting reporters. These nearly identical engineered click beetle luciferases represent an ideal design for dual-luciferase-based assays, because the inhibition profile should reflect a similar SAR. Also, the red and green shifted luminescence will render this reporter less susceptible to optical compound interferences.

The largest series of luciferase inhibitors in this study contained a 2-aryl-substituted benzo- [d]thiazole, -imidazole, and -oxazole cores. Modeling of a benzthiazole inhibitor supported that this type of inhibitor overlaps the same space as the luciferin substrate, and certain substitutions are capable of protruding into the AMP pocket as well. The benzthiazole conforms to a narrow groove created above by Phe249 and below by the C_β of Ala350 and the backbone of Gly343−Leu344. With compound **1g**, the methoxy-phenyl is positioned so that the ether and subsequent carbonyl oxygen can mimic hydrogen bonds observed between the phosphate of AMP and luciferase. This positions the piperizine so that its basic center is in the polar and solvent-exposed phosphate-binding site. Therefore, this type of compound inhibits firefly luciferase by direct competition with luciferin or by an interaction with both the luciferin and AMP pocket, and we noted both modes of inhibition within a series of benzthiazole compounds identified here. In uncharacterized compound collections, such scaffolds should be examined in orthogonal assays to properly assign the activity.

The use of luciferase-based detection for measuring protein kinase activity is a common practice in HTS.[6] Compounds that inhibit via interaction with the ATP-binding site are the most common type of protein kinase inhibitors. Dual inhibitors of luciferases and protein kinases are certainly possible because of the ATP dependence of both enzymes. Such compounds are unlikely to be scored as active because inhibition of both the protein kinase and the luciferase will have opposite effects on the luminescent signal, potentially resulting in false negatives. We identified a series of low MW compounds (<300 Da, compounds **8**−**12**) from the qHTS that have been annotated as protein kinase inhibitors, and these showed inhibition patterns of luciferase that suggest interactions with both the AMP- and luciferin-binding pockets. Flavonoids such as **10**, a known μM MEK inhibitor, have planar structures that can be accommodated in the narrow groove of either kinase or luciferase enzymes. Therefore, dual activity may be common in such compounds, and the luciferase reaction should be measured by using multiple time points, or an alterative assay format should be used to address this issue.[38]

The quinoline/quinazoline core is commonly found in ATP-competitive protein kinase inhibitors, and we identified a series of quinoline-based luciferase inhibitors. We were interested in determining whether our quinoline series could be easily accommodated into the adenosine pocket of protein kinase by using the known protein kinase binding for quinolines. However, in this case, we noted large differences in adenosine binding between protein kinases and luciferase and a clash with the backbone of the gate-keeper residue when attempting to model a representative quinoline-based inhibitor into the adenosine pocket of a typical protein kinase. Therefore, for such larger (>375 daltons) heterocyclic compounds, a different SAR is likely between luciferase and protein kinase inhibitors. Broad-based screening of a publicly available compound collection against protein kinases has not been performed to date, but such information would be extremely useful in further defining the SAR of different ATP-dependent enzymes. Such a data set not only would be useful for identifying potential assay interferences as detailed here but would also aid in understanding the selectivity rules for ATPases in general.

We also identified a large collection of compounds that showed no obvious structural similarity to either ATP or luciferin and noncompetitive inhibition of luciferase; inhibition was not relieved at even high (mM) concentrations of both substrates. This mechanism of action against firefly luciferase was also found for resveratrol, a compound with activity against SIRT1 among other effects.[10]

Although true inhibition of the enzyme reaction through substrate-competitive mechanisms is likely for compounds in which the inhibition can be modulated by variation of substrate concentrations (e.g., the benzthiazolines, which act as luciferin antagonists), nonspecific compound effects on luciferase through mechanisms such as aggregation[39,40] could lead to pseudoinhibition of the enzyme. However, mitigating against this possibility, minimal or no activity was found for most of these apparent noncompetitive inhibitors by using the *P. pennsylvanica* firefly reagent cocktail and the *R. reniformis* luciferase, suggesting specific inhibition of *P. pyralis* luciferase. The presence of 0.01% Tween 20 in the luciferase assay buffer used in our qHTS also implies that compound aggregation is not a predominant mechanism for the luciferase inhibitors identified here, as does the fact that these compounds were often active in reporter gene assays using BrightGlo and SteadyGlo reagents where high (~0.1%) concentrations of detergents such as Triton X-100 are present. Finally, cross-profiling of this luciferase data set versus a qHTS designed to detect detergent-sensitive promiscuous inhibitors[39] confirmed that the compounds discussed here were distinct from those classified as aggregation-based. The database established here should be useful in flagging these types of compounds that will be an issue in HTS, because their inhibition persists even at high substrate concentrations.

Although compound interference based on such nonspecific interactions as aggregation have been described in detail,[39,40] many other causes of assay-related (as opposed to the desired target-related) HTS actives exist, such as fluorescent interference or inhibition of a specific assay component such as the luciferase enzyme described here. The luciferase profile presented here is one of several library characterizations that the NCGC has performed on our publicly available compound collection. We have previously profiled the library for fluorescence[20] and aggregation[39] properties, among others. The amount of activity that we observed for luciferase inhibition (3% of the library) is comparable to interferences obtained by other means, such as fluorescent compound interference. These modes of inhibition can greatly overshadow the actives of interest, which typically represent ~0.1% of the library. For example, in a pyruvate-kinase-luciferase-coupled assay,[11] we noted that more than half of the actives were luciferase inhibitors. The luciferase data set is currently being used to provide a full description of the SAR between these two purine-dependent enzymes. Such detailed descriptions of the chemotypes capable of interfering with common reporters are urgently needed, particularly because public HTS databases grow in size and structural scope. The luciferase data set described here will serve as a useful counter-screen for future luciferase-based HTS assays.

Acknowledgment. This research was supported by the Molecular Libraries Initiative of the NIH Roadmap for Medical Research and the Intramural Research Program of the National Human Genome Research Institute, National Institute of Health. We thank Adam Yasgar and Paul Shinn for compound management support, Sam Michael and Carleen Klumpp for automation assistance, Jeremy Smith for analytical chemistry support, Ryan MacArthur for analysis of PubChem data, and Craig Thomas for critical reading of this manuscript.

Supporting Information Available: Table S1 shows analogues of a coumarin scaffold including compound **18** that were subjected to further assays or identified in the qHTS. Figure S1 shows the firefly luminescence in the presence of lissamine and the dye napthol blue/black and the luminescence from *R. reniformis* in the presence of tartrazine as well as compounds **15** and **16** (at 100 μM). This material is available free of charge via the Internet at http://pubs.acs.org.

References

(1) Wenzel, J. W.; Branham, M. A. The origin of photic behavior and the evolution of sexual communication in fireflies (Coleoptera: Lampyridae). *Cladistics* **2003**, *19*, 1–22.
(2) Ohmiya, Y.; Kjima, S.; Nakamura, M.; Niwa, H. Bioluminescence in Limpet-Like Snail, *Latia neritoides*. *Bull. Chem. Soc. Jpn.* **2005**, *78*, 1197–1205.
(3) Fan, F.; Wood, K. V. Bioluminescent assays for high-throughput screening. *Assay Drug Dev. Technol.* **2007**, *5*, 127–36.
(4) Deluca, M. Firefly luciferase. *Adv. Enzymol. Relat. Areas Mol. Biol.* **1976**, *44*, 37–68.
(5) Nakatsu, T.; Ichiyama, S.; Hiratake, J.; Saldanha, A.; Kobashi, N.; Sakata, K.; Kato, H. Structural basis for the spectral difference in luciferase bioluminescence. *Nature* **2006**, *440*, 372–6.
(6) Inglese, J.; Johnson, R. L.; Simeonov, A.; Xia, M.; Zheng, W.; Austin, C. P.; Auld, D. S. High-throughput screening assays for the identification of chemical probes. *Nat. Chem. Biol.* **2007**, *3*, 466.
(7) Lakowicz, J. R. *Principles of Fluorescence Spectroscopy*; Springer: Berlin, 2006.
(8) Shankar, S.; Singh, G.; Srivastava, R. K. Chemoprevention by resveratrol: Molecular mechanisms and therapeutic potential. *Front. Biosci.* **2007**, *12*, 4839–54.
(9) Blagosklonny, M. V. An anti-aging drug today: From senescence-promoting genes to anti-aging pill. *Drug Discovery Today* **2007**, *12*, 218–224.
(10) Bakhtiarova, A.; Taslimi, P.; Elliman, S. J.; Kosinski, P. A.; Hubbard, B.; Kavana, M.; Kemp, D. M. Resveratrol inhibits firefly luciferase. *Biochem. Biophys. Res. Commun.* **2006**, *351*, 481–484.
(11) Inglese, J.; Auld, D. S.; Jadhav, A.; Johnson, R. L.; Simeonov, A.; Yasgar, A.; Zheng, W.; Austin, C. P. Quantitative high-throughput screening: A titration-based approach that efficiently identifies biological activities in large chemical libraries. *Proc. Natl. Acad. Sci. USA* **2006**, *103*, 11473–8.
(12) http://www.ncbi.nlm.nih.gov/sites/entrez?db=pcsubstance&term=mlsmr.
(13) Yasgar, A.; Shinn, P.; Jadhav, A.; Auld, D. S.; Michael, S.; Zheng, W.; Austin, C. P.; Inglese, J.; Simeonov, A. Compound management for quantitative high-throughput screening. *J. Assoc. Lab. Automation* **2008**, *13*, 79–89.
(14) Cleveland, P. H.; Koutz, P. J. Nanoliter dispensing for uHTS using pin tools. *Assay Drug Dev. Technol.* **2005**, *3*, 213–25.
(15) Sharon, P. M.; Crouch, K.J. S. Methods and kits for detecting protein kinases. U.S. Patent 6911319, 2005.
(16) http://mlsmr.glpg.com.
(17) Stamos, J.; Sliwkowski, M. X.; Eigenbrot, C. Structure of the epidermal growth factor receptor kinase domain alone and in complex with a 4-anilinoquinazoline inhibitor. *J. Biol. Chem.* **2002**, *277*, 46265–72.
(18) Zhang, X.; Gureasko, J.; Shen, K.; Cole, P. A.; Kuriyan, J. An allosteric mechanism for activation of the kinase domain of epidermal growth factor receptor. *Cell* **2006**, *125*, 1137–49.
(19) Eastwood, B. J.; Farmen, M. W.; Iversen, P. W.; Craft, T. J.; Smallwood, J. K.; Garbison, K. E.; Delapp, N. W.; Smith, G. F. The minimum significant ratio: a statistical parameter to characterize the reproducibility of potency estimates from concentration-response assays and estimation by replicate-experiment studies. *J Biomol Screen* **2006**, *11*, 253–61.
(20) Simeonov, A.; Jadhav, A.; Thomas, C. J.; Wang, Y.; Huang, R.; Southall, N.; Shin, P.; Smith J.; Austin, C.P.; Auld, D. S.; Inglese, J. Fluorescent spectroscopic profiling of compound libraries. *J. Med. Chem.* **2008**, this issue.
(21) Ye, L.; Buck, L. M.; Schaeffer, H. J.; Leach, F. R. Cloning and sequencing of a cDNA for firefly luciferase from *Photuris pennsylvanica*. *Biochim. Biophys. Acta* **1997**, *1339*, 39–52.
(22) Hall, M. P.; Gruber, M. G.; Hannah, R. R.; Jennens-Clough M. L.; Wood, K. V. *Stabilization of firefly luciferase using directed evolution*; John Wiley & Sons: New York, 1998.
(23) Branchini, B. R.; Murtiashaw, M. H.; Carmody, J. N.; Mygatt, E. E.; Southworth, T. L. Synthesis of an N-acyl sulfamate analog of luciferyl-AMP: A stable and potent inhibitor of firefly luciferase. *Bioorg. Med. Chem. Lett.* **2005**, *15*, 3860–4.
(24) Boschelli, D. H. 4-Anilino-3-quinolinecarbonitriles: An emerging class of kinase inhibitors. *Curr. Top. Med. Chem.* **2002**, *2*, 1051–63.
(25) Hart, R. C.; Matthews, J. C.; Hori, K.; Cormier, M. J. *Renilla reniformis* bioluminescence: Luciferase-catalyzed production of nonradiating excited states from luciferin analogues and elucidation of the excited state species involved in energy transfer to *Renilla* green fluorescent protein. *Biochemistry* **1979**, *18*, 2204–10.
(26) Burlingham, B.; Widlanski, T. An intuitive look at the relationship of Ki and IC_{50}: A more general use for the Dixon plot. *J. Chem. Educ.* **2003**, *80*, 214–218.
(27) Sun, L. T. N.; Tang, F.; App, H.; Hirth, P.; McMahon, G.; Tang, C. Synthesis and biological evaluations of 3-substituted indolin-2-ones: A novel class of tyrosine kinase inhibitors that exhibit selectivity toward particular receptor tyrosine kinases. *J. Med. Chem.* **1998**, *41*, 2588–2603.
(28) Pietrancosta, N.; Moumen, A.; Dono, R.; Lingor, P.; Planchamp, V.; Lamballe, F.; Bahr, M.; Kraus, J. L.; Maina, F. Imino-tetrahydrobenzothiazole derivatives as p53 inhibitors: discovery of a highly potent in vivo inhibitor and its action mechanism. *J. Med. Chem.* **2006**, *49*, 3645–52.
(29) Dudley, D. T.; Pang, L.; Decker, S. J.; Bridges, A. J.; Saltiel, A. R. A synthetic inhibitor of the mitogen-activated protein kinase cascade. *Proc. Natl. Acad. Sci. USA* **1995**, *92*, 7686–7688.
(30) Alessi, D. R.; Cuenda, A.; Cohen, P.; Dudley, D. T.; Saltiel, A. R. PD 098059 is a specific inhibitor of the activation of mitogen-activated protein kinase kinase in vitro and in vivo. *J. Biol. Chem.* **1995**, *270*, 27489–94.
(31) Ventafridda, V.; Martino, G.; Mandelli, V.; Emanueli, A. Indoprofen, a new analgesic and anti-inflammatory drug in cancer pain. *Clin. Pharmacol. Ther.* **1975**, *17*, 284–9.
(32) Roseth, S.; Fykse, E. M.; Fonnum, F. Uptake of L-glutamate into rat brain synaptic vesicles: effect of inhibitors that bind specifically to the glutamate transporter. *J. Neurochem.* **1995**, *65*, 96–103.
(33) Varney, M. A.; Cosford, N. D.; Jachec, C.; Rao, S. P.; Sacaan, A.; Lin, F. F.; Bleicher, L.; Santori, E. M.; Flor, P. J.; Allgeier, H.; Gasparini, F.; Kuhn, R.; Hess, S. D.; Velicelebi, G.; Johnson, E. C. SIB-1757 and SIB-1893: Selective, noncompetitive antagonists of metabotropic glutamate receptor type 5. *J Pharmacol. Exp. Ther.* **1999**, *290*, 170–81.
(34) Fry, D. W.; Kraker, A. J.; McMichael, A.; Ambroso, L. A.; Nelson, J. M.; Leopold, W. R.; Connors, R. W.; Bridges, A. J. A specific inhibitor of the epidermal growth factor receptor tyrosine kinase. *Science* **1994**, *265*, 1093–5.
(35) Loening, A. M.; Wu, A. M.; Gambhir, S. S. Red-shifted *Renilla reniformis* luciferase variants for imaging in living subjects. *Nat. Meth.* **2007**, *4*, 641–643.
(36) Davis, R. E.; Zhang, Y. Q.; Southall, N.; Staudt, L. M.; Austin, C. P.; Inglese, J.; Auld, D. S. A cell-based assay for IκBα stabilization using a two-color dual luciferase-based sensor. *Assay Drug Dev. Technol.* **2007**, *5*, 85–104.
(37) Almond, B. H. E.; Stecha, P.; Garvin, D.; Paguio, A.; Butler, B.; Beck, M.; Wood, M.; Wood, K. Introducing Chroma-Luc technology. *Promega Notes* **2003**, *85*, 11–14.
(38) Singh, P.; Harden, B. J.; Lillywhite, B. J.; Broad, P. M. Identification of kinase inhibitors by an ATP depletion method. *Assay Drug Dev. Technol.* **2004**, *2*, 161–9.
(39) Feng, B. Y.; Simeonov, A.; Jadhav, A.; Babaoglu, K.; Inglese, J.; Shoichet, B. K.; Austin, C. P. A high-throughput screen for aggregation-based inhibition in a large compound library. *J. Med. Chem.* **2007**, *50*, 2385–90.
(40) McGovern, S. L.; Caselli, E.; Grigorieff, N.; Shoichet, B. K. A common mechanism underlying promiscuous inhibitors from virtual and high-throughput screening. *J. Med. Chem.* **2002**, *45*, 1712–22.

JM701302V